LARGE DEFLECTION OF POINT LOADED CIRCULAR PLATES

by

Allan T. Dolovich

A Thesis

Submitted to the Faculty of Graduate Studies

in Partial Fulfillment of the Requirements for the Degree of

Master of Science

The University of Manitoba

Department of Mechanical Engineering

Winnipeg, Manitoba

ISBN 0-315-34034-7

LARGE DEFLECTION OF POINT LOADED CIRCULAR PLATES

BY

ALLAN T. DOLOVICH

A thesis submitted to the Faculty of Graduate Studies of
the University of Manitoba in partial fulfillment of the requirements
of the degree of

MASTER OF SCIENCE

ABSTRACT

Exact solution of the axisymmetric Von Karman equations for a point loaded clamped circular plate has so far defied all attempts. General expressions which are fairly easy to use are necessary for practical analysis and design applications but few of the existing approximate solutions give the complete behaviour of the plate in an easily used form. A new approximate solution to this problem is herein developed beginning with an assumed model for transverse displacement possessing only one arbitrary constant which allows the plate shape to change. The value of this shape parameter is determined by minimizing a residual formed from the Von Karman equations and the load required to produce a given center deflection is obtained using the principle of virtual work. The new solution consists of very general equations which are relatively easy to use and the present results compare very well with those of existing solutions.

ACKNOWLEDGEMENTS

I would like to take this opportunity to express my heartfelt appreciation and gratitude to Dr. A.B. Thornton-Trump for guiding me through an extremely rewarding Masters program. He has enabled me to achieve goals beyond my most hopeful aspirations.

I would also like to especially thank Dr. Wayne Brodland for suggesting the thesis topic and providing his generous advice and collaborative efforts throughout the completion of this research.

In addition, I am very grateful for numerous conversations with Dr. D. Trim regarding the mathematics associated with my work. It seems he is never too busy to see a willing student.

Thanks are also due to Dr. W. Cleghorn for taking the time to examine my thesis and the Natural Sciences and Engineering Research Council of Canada for the financial assistance it has provided.

Last, but not least, may I thank my parents for teaching me to believe in myself, and my wife Kayla and daughter Ashley for making it all worthwhile.

TABLE OF CONTENTS

LIST OF FIGURES

NOMENCLATURE

A	dimensionless center deflection = w_o/h
a	plate radius
b	parameter in transverse displacement model
C_1, C_2	arbitrary constants
$C_{(i,j)}$	binomial coefficients
c, d	two points a distance dr apart on the same radial line of the middle surface of the plate
cd	original distance between points c and d (before deformation)
$c'd'$	distance between points c and d after loading
D	flexural stiffness of plate = $\frac{Eh^3}{12(1-\mu^2)}$
E	Young's Modulus
e	strain
e^b	strain due to bending
e^m	strain due to membrane effects
$\bar{e}$	dimensionless strain = $\frac{ea^2}{h^2}$
F	functional defined by $\int_{\epsilon}^{1} \lvert X \rvert \, dR$
F_r	total force in the radial direction
F_z	total force in the axial direction
f_1	parameter in expressions for membrane stress, strain, and displacement = $\frac{b(2b-1-\mu)}{b-1}$
f_2	parameter in expressions for membrane stress, strain and displacement = $\frac{8b(b+1-\mu)}{b+2}$

f_3	parameter in expressions for membrane stress, strain, and displacement = $\frac{b^2(3-\mu)}{2}$
h	plate thickness
I_b	"energy terms" due to bending
I_m	"energy terms" due to membrane effects
K	parameter in expressions for membrane stress, strain, and displacement = $\frac{-6(1-\mu^2)A^2}{(b-2)^2}$
k	dummy variable
k_1, k_2	arbitrary constants
ln	natural logarithm
log	logarithm base 10
M_r, M_t	bending stress resultants
m	arbitrary constant
N_r, N_t	normal stress resultants
n	arbitrary constant
P	central point load
$\bar{P}$	dimensionless load = $\frac{Pa^2}{Dh}$
$\bar{P}_S$	expression for load derived by Schmidt
$\bar{P}_{CY}$	expression for load derived by Chien and Yeh
$\bar{P}_V$	expression for load derived by Volmir
p	generic point in the plate
Q_r	shear stress resultant
q	general loading function
q_o	uniform load
R	normalized radial distance from center of the plate = r/a
R_c	inflection point of plate profile

$\bar{R}$	radial body force per unit volume
r	radial coordinate of polar or cylindrical coordinate system
S	stress
S^b, Sb	bending stress
S^m, Sm	membrane stress
$\bar{S}$	dimensionless stress = $\frac{Sa^2h}{D}$
t	as subscript, denotes tangential component in θ direction
U	dimensionless radial displacement due to membrane effects = $\frac{ua}{h^2}$
u_r	radial displacement
$u^b{}_r$	radial displacement due to bending
$u^m{}_r$, u	radial displacement due to membrane effects
V	strain energy
$\bar{V}$	dimensionless strain energy = $\frac{Va^2}{Dh^2}$
$\bar{V}^b$	dimensionless strain energy due to bending only
$\bar{V}^m$	dimensionless strain energy due to membrane effects only
$\bar{V}$	plate volume
W	normalized transverse displacement = w/h
w	transverse displacement
wo	transverse displacement at center of the plate
X	a residual of the Von Karman equation expressing axial equilibrium

Y	first derivative of the dimensionless radial membrane stress with respect to normalized position $R = \frac{d\bar{S}^m_r}{dR}$
Z	normalized axial distance from the middle surface = z/h
$\bar{Z}$	axial body force per unit volume
z	axial coordinate of cylindrical coordinate system
α_r	angle between the tangent to the middle surface and the original r axis
β_r	rotation of normal to middle surface of plate (in r-z plane)
ϵ	a small positive quantity
θ	tangential (angular) coordinate of polar or cylindrical coordinate system
μ	Poisson's ratio
π	Pi, approximately 3.1416
ϕ	stress function
$\sum$	Summation
∇	Vector operator del
∇^2	Laplacian operator = $\nabla \cdot \nabla$
∇^4	biharmonic operator = $\nabla^2 \nabla^2$
∞	infinity
$\cdot$	dot product
$<<$	much less than
$\doteq$	approximately equal to
$\|\|$	absolute value

CHAPTER 1

INTRODUCTION

1.1 PROLOGUE

One of the objectives in the field of solid mechanics is to obtain solutions which describe the behaviour of bodies of various geometries and material properties under different conditions of load and support. However, there is not, as yet, an exact solution for the large deflection of a thin clamped circular plate subjected to a concentrated or point load at its center. Although approximate solutions already exist for this problem, there is not a sufficiently general result which is easy to use and gives all desired quantities. Thus, there is a need for further examination of this case and a new approach may reveal as yet unidentified aspects of the plate's response, thereby leading to a better understanding of the problem as a whole.

1.2 PROBLEM STATEMENT

Consider a thin circular plate of radius a and uniform thickness h subjected to a central point load P as shown in Figure 1.1. The origin of the Lagrangian (undeformed) cylindrical coordinate system is at the center of the plate's middle surface and the plate's material properties

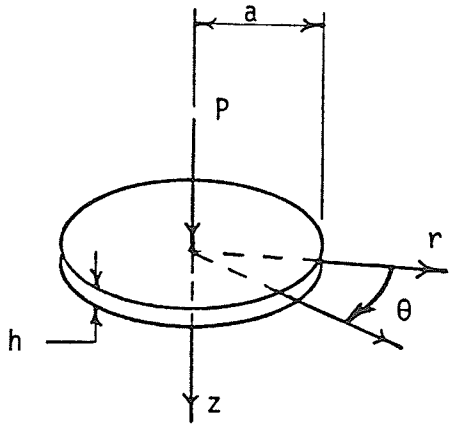

Figure 1.1 Point Loaded Circular Plate

are assumed to be described by Young's modulus E and Poisson's ratio μ. Considerations of dimensional similitude show that the problem may be specified by three independent dimensionless groups [1] and the parameters commonly used in existing analyses of circular plates [2] are a/h, μ, and Pa^2/Dh where D is the flexural stiffness of the plate given by $D = Eh^3/12(1-\mu^2)$. Also, since the load is symmetric with respect to the z axis and the deformation is assumed to be as well, the problem is said to be axisymmetric. All quantities are independent of tangential coordinate θ and the plate's behaviour is governed by a coupled set of ordinary rather than partial differential equations.

The axisymmetric Von Karman equations describe the behaviour of thin circular plates undergoing large lateral deflection but small rotation. A derivation of these coupled, fourth order, nonlinear equations can be found in

Brodland [1]. They are:

$$\nabla^4 w = \frac{1}{D}\left[q + \frac{1}{r}\frac{d^2\phi}{dr^2}\frac{dw}{dr} + \frac{1}{r}\frac{d\phi}{dr}\frac{d^2w}{dr^2}\right] \tag{1.1}$$

$$\nabla^4 \phi = -\frac{Eh}{r}\frac{d^2w}{dr^2}\frac{dw}{dr} \tag{1.2}$$

where lateral displacement w and stress potential ϕ are unknown functions of radial position r, and q(r) is the applied loading distribution. A different but equivalent form of these equations will be derived in chapter 3 and used for the present approach.

In chapter 4 a new approximate solution will be developed for the case of a clamped boundary. This large deflection analysis differs from the so-called linear theory in that the plate changes shape and the difference between the undeformed Lagrangian and deformed Eulerian coordinate systems must be considered. That is, there is an inherent geometric nonlinearity which manifests itself in a nonlinear strain-displacement relation. Membrane effects are now exhibited in addition to bending effects since stretching of the plate's middle surface can no longer be ignored.

However, the analysis which is to follow might be more appropriately termed 'intermediate' deflection theory, since the results do have a particular limited domain over which they are applicable. The Von Karman equations are valid for thin plates with small rotations and center

deflections of the order of plate thickness h*. Also, within this range, local strains are sufficiently small that Hooke's law applies and material linearity is assumed. (Very large plate deflection theory would include large rotations as well as the effects of both geometric and material nonlinearity.) Additional material assumptions include homogeneity and isotropy and the key assumption which facilitates the present analysis is the Kirchhoff hypothesis that a line originally normal to the middle surface of the plate remains perpendicular to it after deformation and does not change in length. This is valid for very thin plates where shearing strain is negligible and the effect of the normal stress S_z can be ignored.

The new scheme to be implemented requires a, h, E, μ, and center deflection w_o as input data. Load P could have been used alternatively in place of w_o, but the present approach lends itself to calculation of the point load required to produce a given center deflection. Solution development begins with an assumed lateral displacement model w which satisfies clamped boundary conditions and possesses only one arbitrary parameter b. Substitution of this form into the 'equivalent' Von Karman equations yields three linear differential equations of which two can be solved simultaneously to obtain expressions for radial and

* Linear deflection theory is valid for center deflections less than one fifth of plate thickness h.

tangential stress. Application of constitutive equations and strain-displacement relations then leads to the determination of strains and radial displacements. Subsequently, an expression for the plate's strain energy is derived and the central load is defined as a function of center deflection, material properties, plate geometry, and parameter b by means of the principle of virtual work. Finally, the value of b for any given set of input data is selected so as to minimize the residual of the third 'equivalent' Von Karman equation. A functional is chosen to map this residual to a real number for each b considered and the optimal value is determined numerically with a single variable search. An accurate empirical form for b is found and the expressions for load, stress, strain, and displacement thereby become known functions of radial position r.

The evaluation of this solution in Chapter 5 will be based on accuracy, generality, usefulness, and range of applicability. In addition, its merit in characterizing the plate's behaviour will be viewed in light of the limiting cases of the present problem. For increasingly large w_o/h the plate response approaches that of a membrane while for very small w_o/h, deflections are in the linear domain. Thus, the present results will be compared to the classical linear theory which is governed by Lagrange's equation

$$\nabla^4 w = \frac{q}{D} \tag{1.3}$$

subject to the boundary conditions

$$w\Big|_{r=a} = 0 \tag{1.4}$$

$$\frac{dw}{dr}\Big|_{r=a} = 0 \tag{1.5}$$

which enforce zero deflection and rotation at the clamped edge of the plate. The resulting small deflection solution is given by

$$w(r) = \frac{P}{16\pi D}\left[2r^2 \ln\frac{r}{a} + a^2 - r^2\right] \tag{1.6}$$

$$w_o = \frac{Pa^2}{16\pi D} \tag{1.7}$$

$$S_r = \frac{3P}{\pi h^3} z\left[(1+\mu)\ln\frac{a}{r} - 1\right] \tag{1.8}$$

and

$$S_t = \frac{3P}{\pi h^3} z\left[(1+\mu)\ln\frac{a}{r} - \mu\right] \tag{1.9}$$

where S_r and S_t are, respectively, the radial and tangential stress. Finally, further insight into the nature of the present solution can be obtained by considering the case analyzed here as part of a more general set of problems. Notably, a circular plate is itself the limiting case of a shallow shell as the shell's radius of curvature becomes infinitely large.

CHAPTER 2

LITERATURE SURVEY

Von Karman [3] derived his famous equations for geometrically nonlinear plate behaviour in 1910. Also, as shown in Figure 2.1, the absence of an exact solution for large deflections of a point loaded plate is accompanied by a lack of experimental work in the available literature. There are, however, approximate solutions which can be evaluated in terms of the criteria

(1) usefulness,
(2) generality,
(3) accuracy, and
(4) range of applicability

where we note that criteria (3) and (4) are closely related; the range of applicability depends on the maximum error which is acceptable.

In 1956, Volmir [4] obtained an approximate solution which has been presented by Timoshenko [5] and Lukasiewicz [6] and which is of the same genre as the present approach but differs in the displacement model chosen and the residual minimization technique used. Here, the assumed displacement model is

$$w = w_o \left(1 - \frac{r^2}{a^2} + \frac{2r^2}{a^2}\ln\frac{r}{a}\right) \qquad (2.1)$$

where w_o, the center deflection, is the only unknown constant to be determined. This expression for lateral

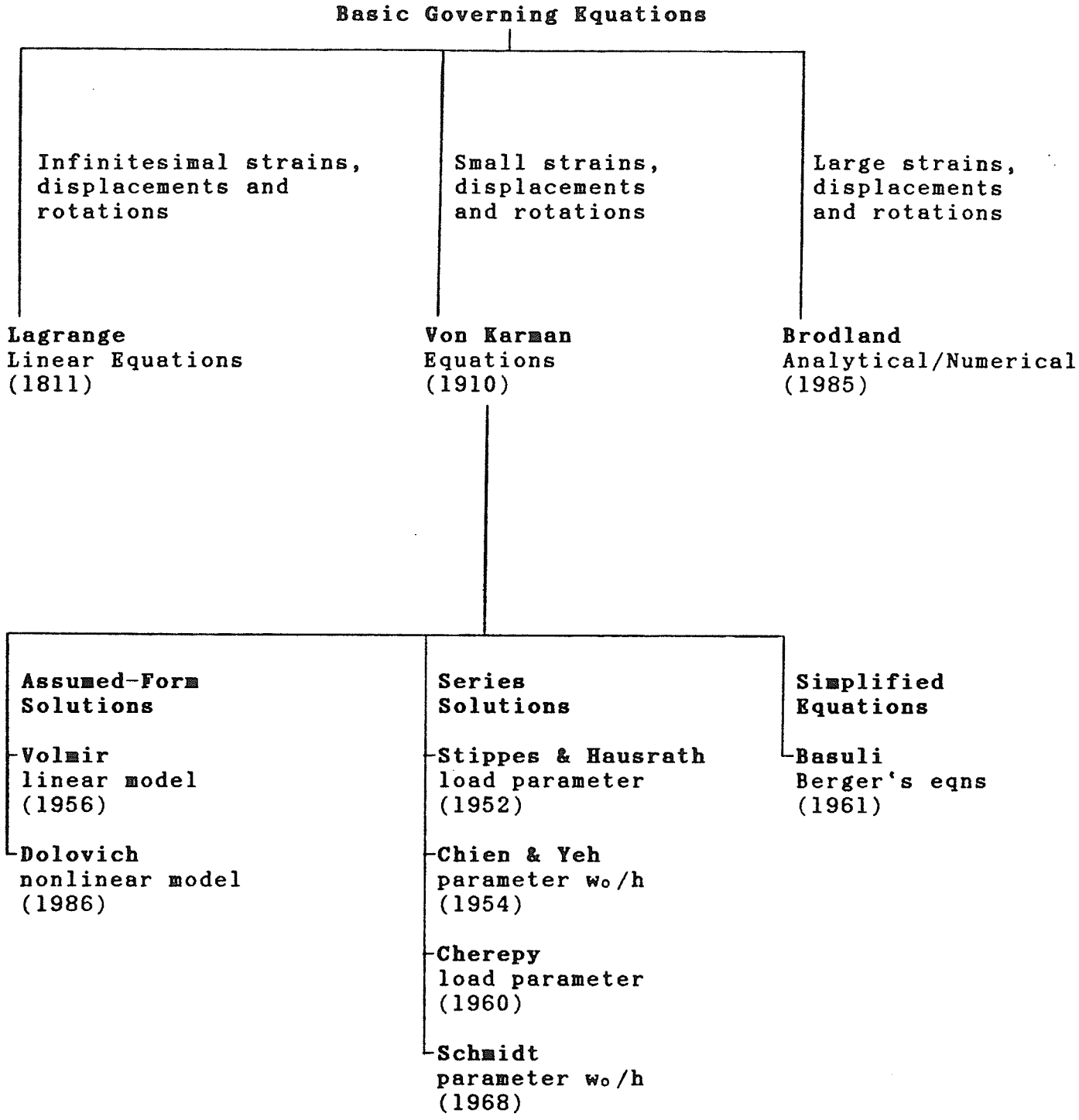

Figure 2.1 Point Loaded Circular Plate Literature

displacement is of the same form as that for the small deflection linear solution [7] and therefore the approach taken assumes that the shape of the plate does not change as deflections increase. The value of w_o for any case is obtained by applying Galerkin's method to minimize a residual formed from substituting one of the Von Karman equations into the other and rearranging. The inner product of this expression with the test function given in (2.1) is subsequently set to zero yielding an algebraic equation which can be solved for the center deflection. This method is shown to be equivalent to the application of Ritz's procedure in order to minimize the total plate strain energy.

Simple explicit expressions are given for the bending and membrane stresses while a general load-deflection relation is produced. However, it should be noted that the displacement model is based on the erroneous assumption that the plate does not change shape. In fact, physical evidence indicates that the point of inflection of a point loaded plate profile changes position as the center deflection increases. Thus, the Volmir approach offers limited insight into the nature of the lateral displacement function for the nonlinear case.

In addition to Ritz-Galerkin methods, a number of perturbation solutions are available in the literature. Stress and displacement are assumed to be representable by power series of a parameter such as load or center

deflection and the unknown coefficients are actually functions which are determined successively by the solution of a recursive set of differential equations.

Cherepy [8] as well as Stippes and Hausrath [9] used dimensionless central load $\overline{P}$ as the perturbation parameter but found that the rate of convergence of the series was poor thus limiting the practical usefulness of the resulting solution.

In contrast, Chien and Yeh [10] have found good success using central normalized deflection. A completely general solution is derived giving simple design formulae for center and edge stresses, central load, and lateral displacement. However, expressions for the membrane stress are long and only two terms for each series are derived. Thus, additional terms would be fairly difficult to obtain as the algebra becomes more involved with the solution of each successive differential equation.

Schmidt [11] has produced a different perturbation solution which is reported in Chia [12] and utilizes power series in w_o/h. Unfortunately, the formulas he presents for load, edge stress, and center stress are valid only for Poisson's ratio equal to 0.3. In addition, the nature of his results are further obscured by the absence of any general expressions for stress, load, and displacement. Thus, his solution is of limited practical usefulness.

A third approach, adopted by Basuli [13] in 1961, involves simplification of the original mathematical

problem by using an altered form of the governing differential equations. In his solution, Basuli uses equations developed by Berger [14] and obtains expressions for lateral deflection and radial displacement which are quite general but require evaluation of the modified Bessel functions in addition to the determination of a parameter " α " by means of an iterative numerical scheme. Also, formulae for stresses are not derived so that the Basuli solution is less than complete and rather difficult to use.

Most recently, Brodland [1] has developed an efficient numerical scheme to analyze the large axisymmetric deformation of thin shells of revolution. His algorithm allows arbitrarily large strains and rotations and gives all desired quantities, but in its published form, is applicable only to incompressible materials; that is, materials possessing a Poisson's ratio of 0.5. Results reported for selected problems including uniformly loaded plates are extremely good so that it will be advantageous to consider and compare information provided for the present case of a point loaded clamped plate.

Finally, it should be noted that solutions to different but associated problems are available in the literature. For example, Jahsman, Field and Holmes [15] have analyzed point loaded membranes while Frakes and Simmonds [16] have produced a perturbation solution for simply supported plates with a Poisson's ratio of 1/3. Also, Saibel and Tadjbakhsh [17] have extended Chien and Yeh's work to

include the effects due to the combined action of uniform lateral pressure and a concentrated central load. However, the greatest attention here will be paid to the analysis of clamped point loaded plates and, consequently, the majority of the discussion to follow will focus on comparison of the present solution to the results of Brodland, Volmir, Schmidt, Basuli, and Chien and Yeh.

CHAPTER 3

GOVERNING EQUATIONS

3.1 ASSUMPTIONS

In this chapter, mathematical development will lead to a derivation of the Von Karman equations. The theory presented here for the large deflection of thin plates is based on the following assumptions [1,7]:

1) The plate is very thin; $h \ll a$.

2) The transverse deflection w is small compared with outer radius a and does not exceed the order of plate thickness h.

3) Rotations are small.

4) The effect of transverse shear is negligible.

5) Normal stresses in a direction perpendicular to the plane of the plate are negligible.

6) Fibers normal to the undeformed middle surface remain normal to it after deformation and do not change length (Kirchhoff's hypothesis).

7) Radial strains are infinitesimal.

8) The material is homogeneous, isotropic, and linearly elastic.

3.2 STRAIN-DISPLACEMENT RELATIONS

As opposed to small deflection theory where strains are due to bending effects only, in the present case, radial strain is due to three sources:

1) Bending,
2) Radial displacement, and
3) Finite rotation of the meridian.

In order to examine the latter two 'membrane effects', consider strains in the middle surface where bending strains $e^b_r = e^b_t = 0$.

Let c and d be two points which are initially a distance dr apart on the same radial line of the middle surface.

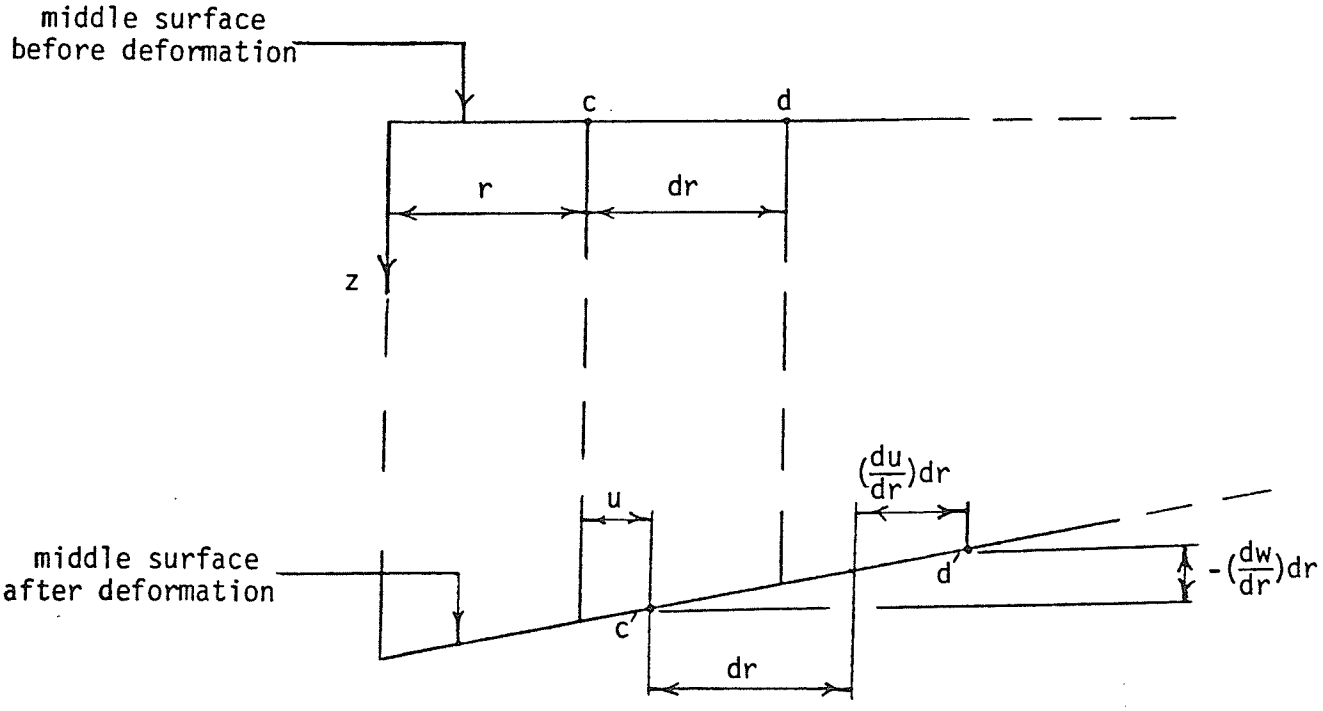

Figure 3.1 Membrane Displacements

As shown in Figure 3.1, $u=u^m{}_r$ is the radial displacement due to stretch and the slope of the deformed middle surface is exaggerated for clarity. Displacement u is measured in the horizontal direction and the redundant symbolism $u^m{}_r=u$ is adopted for convenience since the symbol for radial displacement of the middle surface is to be written quite frequently throughout Chapter 4. Now

$$e^m{}_r = \frac{c'd' - cd}{cd} \tag{3.1}$$

where $e^m{}_r$ = the radial strain in the middle surface

cd = the original distance between points c and d (before deformation) = dr

and $c'd'$ = the distance between points c and d after loading.

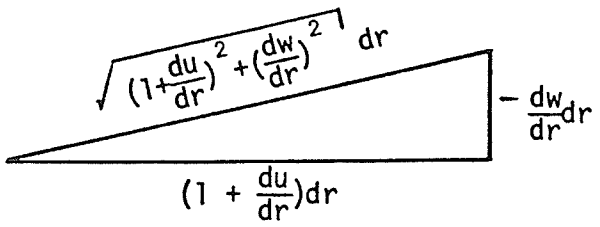

Figure 3.2 Radial Stretch

So, referring to Figures 3.1 and 3.2,

$$e^m_r = \frac{[1 + 2\frac{du}{dr} + \frac{du}{dr}^2 + \frac{dw}{dr}^2]^{1/2} dr - dr}{dr} \tag{3.2}$$

$$= [1 + 2\frac{du}{dr} + \frac{du}{dr}^2 + \frac{dw}{dr}^2]^{1/2} - 1 \tag{3.3}$$

and this can be expanded using the binomial theorem to yield

$$e^m_r = \{\sum_{k=0}^{\infty} C_{(1/2,k)} [2\frac{du}{dr} + \frac{du}{dr}^2 + \frac{dw}{dr}^2]^k\} - 1 \tag{3.4}$$

$$= \frac{du}{dr} + \frac{1}{2}\frac{dw}{dr}^2 - \frac{1}{2}\frac{du}{dr}\frac{dw}{dr}^2 - \frac{1}{2}\frac{du}{dr}^3 + \ldots \tag{3.5}$$

$$= \frac{du}{dr} + \frac{1}{2}\frac{dw}{dr}^2 \tag{3.6}$$

since from assumptions (3) and (7), du/dr is infinitesimal and dw/dr is small. Note that for the classical linearized theory of elasticity,

$$e_r = \frac{du}{dr} \tag{3.7}$$

and the additional term $\frac{1}{2}\frac{dw}{dr}^2$ in Equation (3.6) is due to the added stretching caused by meridian rotation.

The total radial strain e_r at any point in the plate is given by

$$e_r = \frac{d}{dr}(u^b_r + u^m_r) + \frac{1}{2}\frac{dw}{dr}^2 \tag{3.8}$$

where u^b_r is the additional displacement due to bending. Also, from the Kirchhoff hypothesis, a straight line normal to the undeformed middle surface remains perpendicular to it after loading.

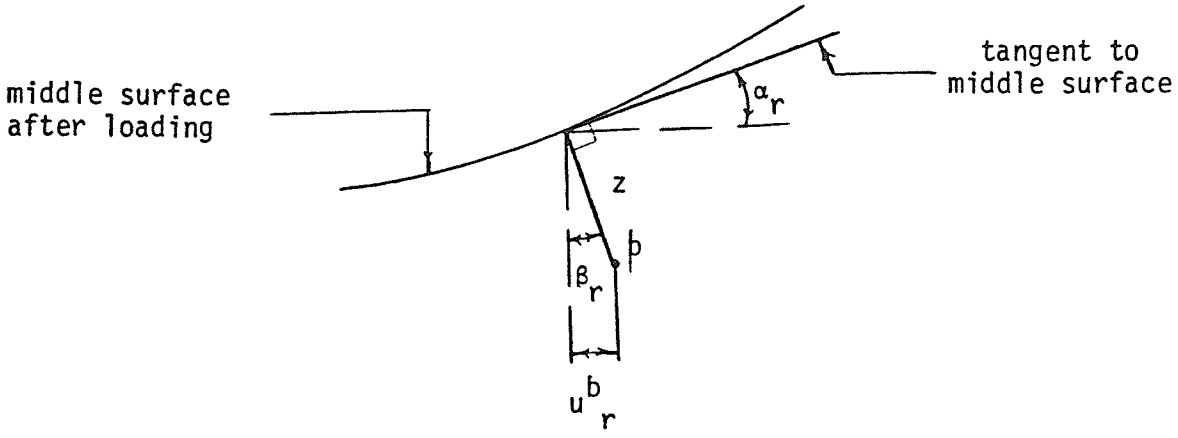

Figure 3.3 Bending Displacements

So for point p an axial distance z from the middle surface as shown in Figure 3.3,

$$\frac{u^b_r}{z} = \sin\beta_r \doteq \beta_r = \alpha_r \doteq -\frac{dw}{dr} \qquad (3.9)$$

or

$$u^b_r = -z\,\frac{dw}{dr} \qquad (3.10)$$

where rotations are assumed small as per assumption (3). Consequently, from Equation (3.8),

$$e_r = -z\,\frac{d^2w}{dr^2} + \frac{du}{dr} + \frac{1}{2}\left(\frac{dw}{dr}\right)^2 \qquad (3.11)$$

$$= e^b_r + e^m_r \qquad (3.12)$$

where e^b_r is the radial strain due to bending.

An expression for the transverse strain e_t can be obtained by examining the deformation of arc ij as shown in Figure 3.4.

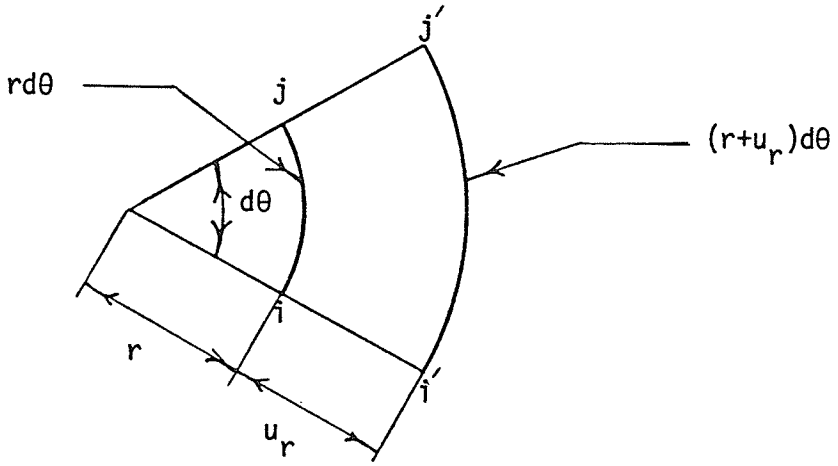

Figure 3.4 Transverse Strain

$$e_t = \frac{(r+u_r)d\theta - rd\theta}{rd\theta} \tag{3.13}$$

$$= \frac{u_r}{r} \tag{3.14}$$

but

$$u_r = u^b_r + u^m_r \tag{3.15}$$

$$= -z\,\frac{dw}{dr} + u\ . \tag{3.16}$$

So the total transverse strain is given by

$$e_t = -\frac{z}{r}\frac{dw}{dr} + \frac{u}{r} . \qquad (3.17)$$

3.3 CONSTITUTIVE RELATIONS

In cylindrical coordinates, generalized Hooke's law [7] can be written as

$$e_r = \frac{1}{E}(S_r - \mu S_t - \mu S_z) \qquad (3.18)$$

$$e_t = \frac{1}{E}(-\mu S_r + S_t - \mu S_z) \qquad (3.19)$$

$$e_z = \frac{1}{E}(-\mu S_r - \mu S_t + S_z) \qquad (3.20)$$

where e_z is the axial normal strain and S_r, S_t, and S_z are respectively the radial, tangential, and axial normal stress. Assuming that $S_z = 0$ as per assumption (5), Equations (3.18) and (3.19) can be simplified and inverted to give

$$S_r = \frac{E}{1-\mu^2}(e_r + \mu e_t) \qquad (3.21)$$

and

$$S_t = \frac{E}{1-\mu^2}(\mu e_r + e_t) \qquad (3.22)$$

so that substitution of Equations (3.11) and (3.17) for

strain into (3.21) and (3.22) yields

$$S_r = \frac{E}{1-\mu^2}\left\{\left[\frac{du}{dr} + \frac{1}{2}\left(\frac{dw}{dr}\right)^2 + \mu\frac{u}{r}\right] - z\left[\frac{d^2w}{dr^2} + \frac{\mu}{r}\frac{dw}{dr}\right]\right\} \tag{3.23}$$

and

$$S_t = \frac{E}{1-\mu^2}\left\{\left[\frac{u}{r} + \mu\frac{du}{dr} + \frac{\mu}{2}\left(\frac{dw}{dr}\right)^2\right] - z\left[\frac{1}{r}\frac{dw}{dr} + \mu\frac{d^2w}{dr^2}\right]\right\} \tag{3.24}$$

or

$$S_r = S^m{}_r + S^b{}_r \tag{3.25}$$

$$S_t = S^m{}_t + S^b{}_t \tag{3.26}$$

where

$$S^m{}_r = \frac{E}{1-\mu^2}\left[\frac{du}{dr} + \frac{1}{2}\left(\frac{dw}{dr}\right)^2 + \mu\frac{u}{r}\right] \tag{3.27}$$

$$S^m{}_t = \frac{E}{1-\mu^2}\left[\frac{u}{r} + \mu\frac{du}{dr} + \frac{\mu}{2}\left(\frac{dw}{dr}\right)^2\right] \tag{3.28}$$

$$S^b{}_r = \frac{-Ez}{1-\mu^2}\left[\frac{d^2w}{dr^2} + \frac{\mu}{r}\frac{dw}{dr}\right] \tag{3.29}$$

and

$$S^b{}_t = -\frac{Ez}{1-\mu^2}\left[\frac{1}{r}\frac{dw}{dr} + \mu\frac{d^2w}{dr^2}\right] . \tag{3.30}$$

3.4 STRESS RESULTANTS

The stress distributions over the transverse faces of a plate element can be reduced to moments and forces per

unit circumferential length acting at the middle surface. These moments and forces are called stress resultants. Specifically, the bending stress resultants are given by

$$M_r = \int_{-h/2}^{h/2} zS_r \, dz \tag{3.31}$$

$$M_t = \int_{-h/2}^{h/2} zS_t \, dz \tag{3.32}$$

while the normal stress resultants are

$$N_r = \int_{-h/2}^{h/2} S_r \, dz \tag{3.33}$$

$$N_t = \int_{-h/2}^{h/2} S_t \, dz \tag{3.34}$$

and the shear force stress resultant is

$$Q_r = \int_{-h/2}^{h/2} S_{rz} \, dz \tag{3.35}$$

where S_{rz} is the transverse shear stress. Note that the plate is assumed to carry shear stress but as indicated in

assumption (4) does not undergo shear strain as a result. This apparent incompatability is however reasonable in thin plates where shear deformations are negligible even though shear stress resultants are not.

N_r, N_t, M_r and M_t can be written in terms of radial and lateral displacements by substituting expressions (3.23) and (3.24) for stress into Equations (3.31) through (3.34) yielding

$$M_r = -D\left[\frac{d^2w}{dr^2} + \frac{\mu}{r}\frac{dw}{dr}\right] = \frac{h^3}{12z} S^b{}_r \qquad (3.36)$$

$$M_t = -D\left[\frac{1}{r}\frac{dw}{dr} + \mu\frac{d^2w}{dr^2}\right] = \frac{h^3}{12z} S^b{}_t \qquad (3.37)$$

$$N_r = \frac{Eh}{1-\mu^2}\left[\frac{du}{dr} + \frac{1}{2}\frac{dw}{dr}^2 + \mu\frac{u}{r}\right] = hS^m{}_r \qquad (3.38)$$

and

$$N_t = \frac{Eh}{1-\mu^2}\left[\frac{u}{r} + \mu\frac{du}{dr} + \frac{\mu}{2}\frac{dw}{dr}^2\right] = hS^m{}_t \ . \qquad (3.39)$$

Stress resultants will play an important role in both the consideration of static plate equilibrium and the derivation of the governing differential equations. In fact, N_r, N_t, and displacement w are the three unknown functions in the equivalent Von Karman equations to be obtained in Section 3.6.

3.5 EQUILIBRIUM EQUATIONS

Consider the element in Figure 3.5 where the slope at r is dw/dr and the slope at r+dr is $\frac{dw}{dr} + \frac{d}{dr}\left(\frac{dw}{dr}\right)dr$

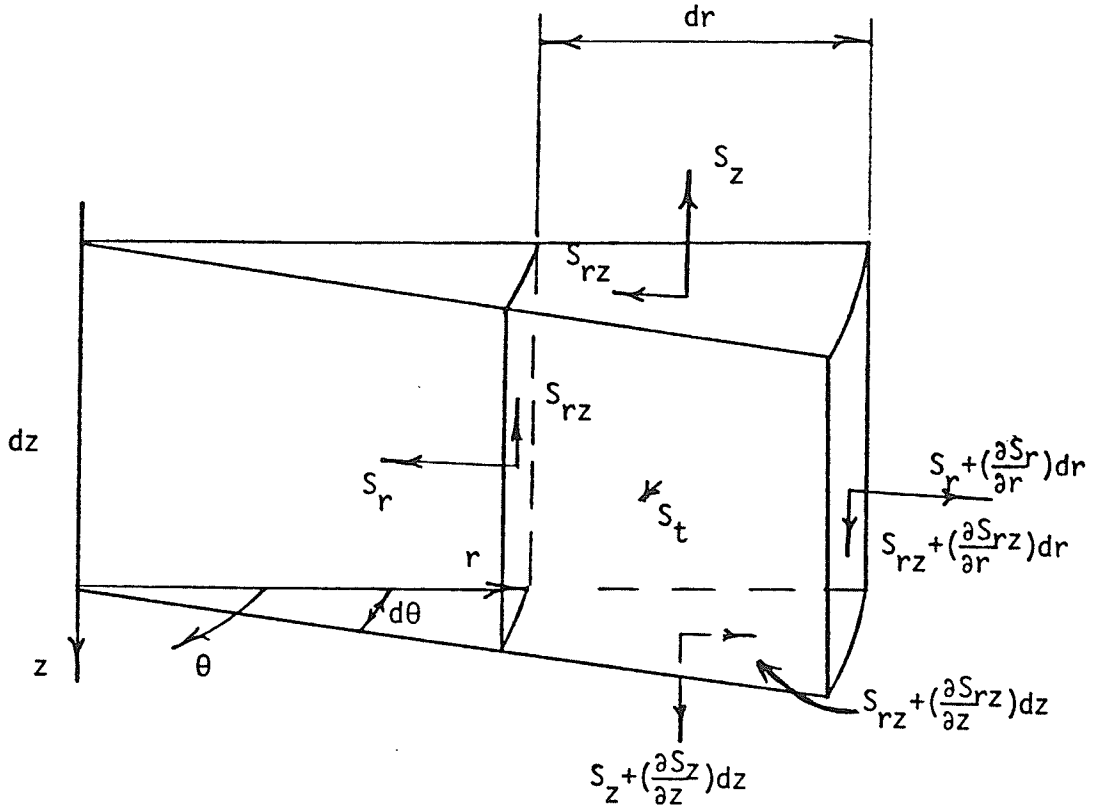

Figure 3.5 Volumetric Element

For static equilibrium in the radial direction,

$$\sum F_r = 0 = [S_{rz}+\frac{\partial S_{rz}}{\partial z}\,dz][rdrd\theta]-[S_{rz}][rdrd\theta]$$
$$+ [S_r+\frac{\partial S_r}{\partial r}dr][(r+dr)d\theta dz] - [S_r][rd\theta dz]$$
$$- [2S_t\frac{d\theta}{2}][drdz] + \bar{R}rdrd\theta dz \qquad (3.40)$$

where $S_t\,d\theta/2$ is the radial component of S_t due to the geometry of the element and $\bar{R}$ is the radial body force per unit volume.

Rearranging and dividing Equation (3.40) by element volume $rdrd\theta dz$ yields

$$\frac{\partial S_r}{\partial r} + \frac{S_r-S_t}{r} + \frac{\partial S_{rz}}{\partial z} + \bar{R} = 0 \qquad (3.41)$$

while integrating (3.41) with respect to dz from - h/2 to h/2 gives

$$\frac{dN_r}{dr} + \frac{N_r-N_t}{r} + S_{rz}\Big|_{-h/2}^{h/2} + \int_{-h/2}^{h/2}\bar{R}dz = 0 \qquad (3.42)$$

where $\int_{-h/2}^{h/2}\bar{R}dz$ = the total radial body force per unit area of middle surface

and $S_{rz}\Big|_{-h/2}^{h/2}$ = the total radial traction force per unit area of middle surface.

Alternatively, integrating Equation (3.41) with respect to zdz from -h/2 to h/2 gives

$$\frac{dM_r}{dr} + \frac{M_r - M_t}{r} + \int_{-h/2}^{h/2} z\frac{\partial S_{rz}}{\partial z}dz + \int_{-h/2}^{h/2} z\bar{R}dz = 0 \qquad (3.43)$$

or, after applying integration by parts to the third term,

$$\frac{dM_r}{dr} + \frac{M_r - M_t}{r} - Q_r + \int_{-h/2}^{h/2} z\bar{R}dz + zS_{rz}\Big|_{-h/2}^{h/2} = 0 \qquad (3.44)$$

where $\int_{-h/2}^{h/2} z\bar{R}dz + zS_{rz}\Big|_{-h/2}^{h/2}$ = the total applied moment per unit area of middle surface.

Also, in the absence of radial surface tractions and body forces, Equations (3.42) and (3.44) become respectively

$$\frac{dN_r}{dr} + \frac{N_r - N_t}{r} = 0 \qquad (3.45)$$

and

$$\frac{dM_r}{dr} + \frac{M_r - M_t}{r} = Q_r \ . \qquad (3.46)$$

Finally, consider that part of the plate from the center to r, as shown in Figure 3.6, and only those stress resultants contributing to axial reaction.

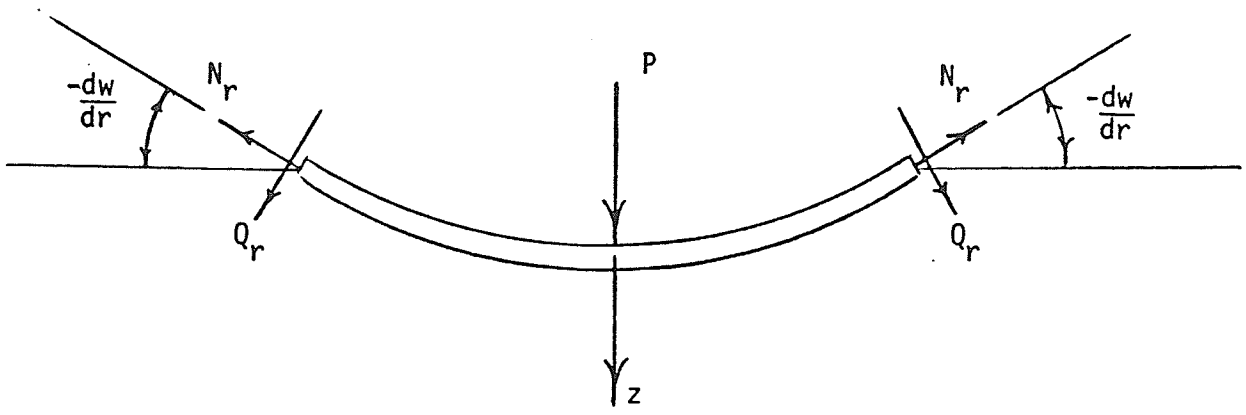

Figure 3.6 Plate Element

For static equilibrium, in the axial direction

$$\sum F_z = 0 = P - N_r\left(-\frac{dw}{dr}\right)(2\pi r) + Q_r(2\pi r) \qquad (3.47)$$

or

$$-Q_r = \frac{P}{2\pi r} + N_r \frac{dw}{dr} . \qquad (3.48)$$

3.6 THE VON KARMAN EQUATIONS

With the exception of Equations (3.47) and (3.48), developments have thus far followed Brodland's derivation of the Von Karman equations [1, Chapter 4]. We shall now, however, diverge to obtain the equivalent form used by Way [18] in his analysis of large deflections due to uniform loads.

Substitution of Equations (3.36) and (3.37) into (3.46) gives an expression for shearing reaction Q_r:

$$Q_r = -D\left[\frac{d^3w}{dr^3} + \frac{1}{r}\frac{d^2w}{dr^2} - \frac{1}{r^2}\frac{dw}{dr}\right] \tag{3.49}$$

$$= -D\,\frac{d}{dr}\left[\frac{1}{r}\frac{d}{dr}\left(r\frac{dw}{dr}\right)\right] \tag{3.50}$$

where D is the flexural rigidity of the plate given by $Eh^3/12(1-\mu^2)$. Consequently, axial equilibrium can be expressed by

$$D\,\frac{d}{dr}\left[\frac{1}{r}\frac{d}{dr}\left(r\frac{dw}{dr}\right)\right] = \frac{P}{2\pi r} + N_r\frac{dw}{dr}\,. \tag{3.51}$$

Now, from the definition of tangential membrane strain,

$$u = r\,e^m{}_t \tag{3.52}$$

$$\frac{du}{dr} = e^m{}_t + r\,\frac{de^m{}_t}{dr} \tag{3.53}$$

and substituting into (3.6) gives

$$e^m{}_r = e^m{}_t + r\,\frac{de^m{}_t}{dr} + \frac{1}{2}\left(\frac{dw}{dr}\right)^2\,. \tag{3.54}$$

But, in light of Equations (3.38) and (3.39), the constitutive relations can be written as

$$e^m{}_r = \frac{1}{Eh}\left(N_r - \mu N_t\right) \tag{3.55}$$

$$e^m{}_t = \frac{1}{Eh}\left(-\mu N_r + N_t\right)\,. \tag{3.56}$$

So, substituting (3.55) and (3.56) into (3.54) gives

$$-(1+\mu)N_r + (1+\mu)N_t - \mu r \frac{dN_r}{dr} + r \frac{dN_t}{dr} + \frac{Eh}{2} \frac{dw}{dr}^2 = 0 \ . \qquad (3.57)$$

Also, multiplying Equation (3.45) by r and rearranging yields

$$\frac{d}{dr}(rN_r) - N_t = 0 \qquad (3.58)$$

or

$$N_r = -r \frac{dN_r}{dr} + N_t \qquad (3.59)$$

so that from substitution of (3.59) into the first term of (3.57) we obtain

$$r \frac{d}{dr}(N_r + N_t) + \frac{Eh}{2} \frac{dw}{dr}^2 = 0 \ . \qquad (3.60)$$

Together, Equations (3.51), (3.58) and (3.60) form an equivalent set of axisymmetric Von Karman equations. That is,

$$D \frac{d}{dr}\left[\frac{1}{r} \frac{d}{dr}\left(r \frac{dw}{dr}\right)\right] = \frac{P}{2\pi r} + N_r \frac{dw}{dr} \qquad (3.51)$$

$$\frac{d}{dr}(rN_r) - N_t = 0 \qquad (3.58)$$

$$r \frac{d}{dr}(N_r + N_t) + \frac{Eh}{2} \frac{dw}{dr}^2 = 0 \qquad (3.60)$$

where (3.51) and (3.58) enforce axial and radial

equilibrium respectively and (3.60) is a compatibility relation. If Equation (3.58) is rearranged to give N_t explicitly and is then substituted into (3.60), by defining a stress potential function ϕ such that

$$N_r = \frac{1}{r}\frac{d\phi}{dr} \tag{3.61}$$

$$N_t = \frac{d^2\phi}{dr^2} \tag{3.62}$$

and differentiating once with respect to r, we obtain

$$\nabla^4\phi = -\frac{Eh}{r}\frac{d^2w}{dr^2}\frac{dw}{dr} . \tag{1.2}$$

Similarly, substituting (3.61) and (3.62) into (3.51) yields

$$\nabla^4 w = \frac{1}{D}\left[q + \frac{1}{r}\frac{d^2\phi}{dr^2}\frac{dw}{dr} + \frac{1}{r}\frac{d\phi}{dr}\frac{d^2w}{dr^2}\right] \tag{1.1}$$

and Equations (1.1) and (1.2) are the form of governing equations originally derived by Von Karman [3].

The problem can be given in dimensionless form by writing (3.51), (3.58), and (3.60) as

$$\frac{d}{dR}\left[\frac{1}{R}\frac{d}{dR}\left(R\frac{dW}{dR}\right)\right] = \frac{\bar{P}}{2\pi R} + \bar{S}^m{}_r\frac{dW}{dR} \tag{3.63}$$

$$\frac{d}{dR}\left(R\,\bar{S}^m{}_r\right) - \bar{S}^m{}_t = 0 \tag{3.64}$$

$$R \frac{d}{dR}(\bar{S}^m_r + \bar{S}^m_t) + 6(1-\mu^2) \frac{dW}{dR}^2 = 0 \qquad (3.65)$$

where

$$W = w/h \qquad (3.66)$$

$$R = r/a \qquad (3.67)$$

$$\bar{P} = \frac{Pa^2}{Dh} \qquad (3.68)$$

$$\bar{S}^m_r = \frac{S^m_r a^2 h}{D} = \frac{N_r a^2}{D} \qquad (3.69)$$

$$\bar{S}^m_t = \frac{S^m_t a^2 h}{D} = \frac{N_t a^2}{D} \qquad (3.70)$$

and the associated dimensionless boundary conditions for a clamped plate are:

$$W\Big|_{R=1} = 0 \qquad (3.71)$$

$$\frac{dW}{dr}\Big|_{R=1} = 0 \qquad (3.72)$$

and

$$U\Big|_{R=1} = 0 \qquad (3.73)$$

where $U = \frac{ua}{h^2}$.

CHAPTER 4

A NEW APPROXIMATE SOLUTION

4.1 DISPLACEMENT MODEL

The approximate solution developed in this chapter begins with an assumed nonlinear form for transverse displacement which possesses only one arbitrary constant b. Stresses are subsequently derived so as to satisfy Von Karman equation (1.2) exactly while the value of parameter b is selected so as to minimize a residual formed from the second Von Karman equation given by (1.1). The effectiveness of the present approach depends largely on how well the chosen expression for displacement models the actual plate deflections. Let

$$W = \frac{A}{n}(R^b - mR^2 + n) \tag{4.1}$$

where b, m, n, and A are arbitrary constants. Enforcing zero lateral displacement at the edge of the plate yields

$$n = m - 1 \tag{4.2}$$

while zero slope at R=1 requires that

$$m = b/2 \tag{4.3}$$

and

$$n = \frac{b-2}{2} . \tag{4.4}$$

That is, the final displacement model is given by

$$W = \frac{A}{b-2}\,(2R^b - bR^2 + b - 2)\ . \tag{4.5}$$

Note that

$$W\Big|_{R=0} = A \tag{4.6}$$

which is the central normalized deflection of the plate and is assumed to be known. Hence, b is the only constant which must be determined given values for a, h, E, μ, and A.

Also, expression (4.5) possesses some very useful characteristics. Consider

$$\lim_{b\to 2} W = \{\lim_{b\to 2} 2AR^2\ [\frac{R^{b-2}-1}{b-2} + \frac{1}{b-2} - \frac{b}{2(b-2)}]\} + A \tag{4.7}$$

$$= 2AR^2\ \{\ [\lim_{b\to 2}\ (\frac{R^{b-2}-1}{b-2})] - \frac{1}{2}\ \} + A\ . \tag{4.8}$$

Using l'Hopital's rule and rearranging,

$$\lim_{b\to 2} W = A\ (2R^2 \ln R - R^2 + 1) \tag{4.9}$$

and this is the classical linear solution for deflections of a point loaded clamped plate. That is, expression (4.5) approaches the linear solution as b approaches 2. In addition, the use of only one 'governing' parameter leads to a final solution which is easy to apply. (A simple empirical relation for b will be possible after the nature

of this variable has been investigated.) Finally, note that for the first term in the displacement model, b is the exponent of R. This allows the plate's meridian to change shape with increasing deflection. The resulting characterization of nonlinear point loaded plate behaviour constitutes an improvement over that provided by Volmir's linear form. If we denote by R_c the normalized radial position of the plate meridian's point of inflection, then by setting the second derivative of (4.5) to zero we obtain

$$R_c = (b - 1)^{1/(2-b)} . \tag{4.10}$$

4.2 DERIVED QUANTITIES

The normalized functions for u(r), w(r), and their derivatives make up the integrand of the energy integral which is the basis of analysis in the next section. Thus, an expression for radial displacement of the middle surface u will be derived first.

Recall from equations (3.64) and (3.65) that

$$\bar{S}^m{}_t = \bar{S}^m{}_r + R \frac{d\bar{S}^m{}_r}{dR} \tag{4.11}$$

and

$$R \frac{d}{dR} [\bar{S}^m{}_r + \bar{S}^m{}_t] + 6(1-\mu^2) \frac{dW}{dR}^2 = 0 . \tag{4.12}$$

Substitution of (4.11) and displacement model (4.5) into (4.12) yields

$$R^2 \frac{d^2\bar{S}^m{}_r}{dR^2} + 3R \frac{d\bar{S}^m{}_r}{dR} = \frac{-6(1-\mu^2)A^2}{(b-2)^2} (4b^2R^{2b-2} - 8b^2R^b + 4b^2R^2) \qquad (4.13)$$

and this is a second-order differential equation which can be reduced to two first-order differential equations by letting

$$Y = \frac{d\bar{S}^m{}_r}{dR} \qquad (4.14)$$

so that (4.13) becomes

$$\frac{dY}{dR} + \frac{3Y}{R} = K(4b^2R^{2b-4} - 8b^2R^{b-2} + 4b^2) \qquad (4.15)$$

where

$$K = \frac{-6(1-\mu^2)A^2}{(b-2)^2} . \qquad (4.16)$$

To solve this linear first-order differential equation, we multiply through by integrating factor R^3 giving [19]

$$\frac{d}{dR}(R^3Y) = K(4b^2R^{2b-1} - 8b^2R^{b+1} + 4b^2R^3) \qquad (4.17)$$

and then integrate both sides with respect to dR to obtain

$$Y = K\left(2bR^{2b-3} - \frac{8b^2R^{b-1}}{b+2} + b^2R\right) + \frac{C_1}{R^3} \qquad (4.18)$$

where C_1 is an arbitrary constant and $b \neq 0$, $b \neq -2$. Finally, substitution of (4.18) into (4.14) followed by integration

yields

$$\bar{S}^m{}_r = K\left(\frac{bR^{2b-2}}{b-1} - \frac{8bR^b}{b+2} + \frac{b^2R^2}{2}\right) - \frac{C_1}{2R^2} + C_2 \qquad (4.19)$$

where C_2 is a second arbitrary constant and $b\neq -2$, $b\neq 0$, and $b\neq 1$. $\bar{S}^m{}_t$ can be obtained from (4.11) which gives

$$\bar{S}^m{}_t = K\left[\frac{b(2b-1)R^{2b-2}}{b-1} - \frac{8b(b+1)R^b}{b+2} + \frac{3b^2R^2}{2}\right] + \frac{C_1}{2R^2} + C_2 \qquad (4.20)$$

while substituting (4.19) and (4.20) into Hooke's law gives

$$\bar{e}^m{}_t = \frac{K}{12(1-\mu^2)}\left(f_1R^{2b-2} - f_2R^b + f_3R^2\right) + \frac{C_1R^{-2}}{24(1-\mu)} + \frac{C_2}{12(1+\mu)} \qquad (4.21)$$

where

$$\bar{e}^m{}_t = \frac{a^2}{h^2}\, e_t{}^m \qquad (4.22)$$

$$f_1 = \frac{b(2b-1-\mu)}{b-1} \qquad (4.23)$$

$$f_2 = \frac{8b(b-\mu+1)}{b+2} \qquad (4.24)$$

and

$$f_3 = \frac{b^2(3-\mu)}{2}\ . \qquad (4.25)$$

Now, if we define dimensionless radial displacement U as

$$U = \frac{ua}{h^2} , \tag{4.26}$$

then

$$\bar{e}^m{}_t = \frac{U}{R} \tag{4.27}$$

and

$$U = \frac{K}{12(1-\mu^2)} (f_1 R^{2b-1} - f_2 R^{b+1} + f_3 R^3) + \frac{C_1 R^{-1}}{24(1-\mu)} + \frac{C_2 R}{12(1+\mu)} . \tag{4.28}$$

But we know that $U|_{R=0}$ is finite (and equal to zero). Therefore

$$C_1 = 0 \tag{4.29}$$

and

$$U = \frac{K}{12(1-\mu^2)} (f_1 R^{2b-1} - f_2 R^{b+1} + f_3 R^3) + \frac{C_2 R}{12(1+\mu)} . \tag{4.30}$$

Also, for a clamped plate,

$$U\Big|_{R=1} = 0 \tag{4.31}$$

so

$$C_2 = \frac{K}{\mu-1} (f_1 - f_2 + f_3) \tag{4.32}$$

and finally

$$U = \frac{K}{12(1-\mu^2)} (f_1 R^{2b-1} - f_2 R^{b+1} + f_3 R^3 - f_1 R + f_2 R - f_3 R) . \quad (4.33)$$

Expressions for dimensionless stress and strain can now be written in terms of the original displacement model. Substituting (4.29) and (4.32) into (4.19) yields

$$\bar{S}^m{}_r = K \left(\frac{bR^{2b-2}}{b-1} - \frac{8bR^b}{b+2} + \frac{b^2R^2}{2} + \frac{f_1-f_2+f_3}{\mu-1}\right) \quad (4.34)$$

while from (4.20),

$$\bar{S}^m{}_t = K \left[\frac{b(2b-1)R^{2b-2}}{b-1} - \frac{8b(b+1)R^b}{b+2} + \frac{3b^2R^2}{2} + \frac{f_1-f_2+f_3}{\mu-1}\right] . \quad (4.35)$$

Hooke's law in conjunction with (4.34) and (4.35) gives

$$\bar{e}^m{}_r = \frac{K}{12(1-\mu^2)} \left[\frac{b(-2\mu b+\mu+1)R^{2b-2}}{b-1} - \frac{8b(-\mu b-\mu+1)R^b}{b+2} + \frac{b^2(1-3\mu)R^2}{2} - f_1 + f_2 - f_3\right] \quad (4.36)$$

and equation (4.21) can now be written as

$$\bar{e}^m{}_t = \frac{K}{12(1-\mu^2)} (f_1 R^{2b-2} - f_2 R^b + f_3 R^2 - f_1 + f_2 - f_3) . \quad (4.37)$$

Bending stresses and strains are obtained by substituting displacement model (4.5) into the previously derived relations

$$\bar{S}^b{}_r = -12Z \left[\frac{d^2W}{dR^2} + \frac{\mu}{R}\frac{dW}{dR}\right] \tag{4.38}$$

$$\bar{S}^b{}_t = -12Z \left[\frac{1}{R}\frac{dW}{dR} + \mu\frac{d^2W}{dR^2}\right] \tag{4.39}$$

$$\bar{e}^b{}_r = -Z\frac{d^2W}{dR^2} \tag{4.40}$$

and

$$\bar{e}^b{}_t = -\frac{Z}{R}\frac{dW}{dR} \tag{4.41}$$

where $Z=z/h$ and all dimensional quantities have been replaced with their dimensionless counterparts. Consequently,

$$\bar{S}^b{}_r = \frac{-24bAZ}{b-2}\left[(b-1+\mu)R^{b-2} - 1 - \mu\right] \tag{4.42}$$

$$\bar{S}^b{}_t = \frac{-24bAZ}{b-2}\left[(\mu b-\mu+1)R^{b-2} - 1 - \mu\right] \tag{4.43}$$

$$\bar{e}^b{}_r = \frac{-2bAZ}{b-2}\left[(b-1)R^{b-2} - 1\right] \tag{4.44}$$

and

$$\bar{e}^b{}_t = \frac{-2bAZ}{b-2}\left[R^{b-2} - 1\right] . \tag{4.45}$$

4.3 LOAD DEFLECTION RELATION

Determination of central load P as well as parameter b requires that the expression for strain energy V be known. This is given by

$$V = \iiint_{\forall} \left[\frac{1}{2} S_r e_r + \frac{1}{2} S_t e_t \right] d\forall \tag{4.46}$$

or, in dimensionless form,

$$\bar{V} = \int_0^{2\pi} \int_0^{1} \int_{-1/2}^{1/2} \left[\frac{1}{2} \bar{S}_r \bar{e}_r + \frac{1}{2} \bar{S}_t \bar{e}_t \right] R dZ dR d\theta \tag{4.47}$$

where

$$\bar{V} = \frac{Va^2}{Dh^2} . \tag{4.48}$$

Also, from Hooke's law,

$$\bar{S}_r = 12(\bar{e}_r + \mu \bar{e}_t) \tag{4.49}$$

$$\bar{S}_t = 12(\mu \bar{e}_r + \bar{e}_t) \tag{4.50}$$

so (4.47) can be written as

$$\bar{V} = 6 \int_0^{2\pi} \int_0^{1} \int_{-1/2}^{1/2} \left[\bar{e}_r^2 + \bar{e}_t^2 + 2\mu \bar{e}_r \bar{e}_t \right] R dZ dR d\theta \tag{4.51}$$

and nondimensionalizing expressions (3.11) and (3.17) for

strain, substituting into (4.51) and then integrating with respect to dZ and dθ yields

$$\bar{V} = \bar{V}^b + \bar{V}^m \tag{4.52}$$

where

$$\bar{V}^b = \pi \int_0^1 \left[R \frac{d^2W}{dR^2}^2 + \frac{1}{R} \frac{dW}{dR}^2 + 2\mu \frac{dW}{dR} \frac{d^2W}{dR^2} \right] dR \tag{4.53}$$

and

$$\bar{V}^m = 12\pi \int_0^1 \left[R \frac{dU}{dR}^2 + R \frac{dU}{dR} \frac{dW}{dR}^2 + \frac{R}{4} \frac{dW}{dR}^4 + \frac{U^2}{R} + 2\mu U \frac{dU}{dR} + \mu U \frac{dW}{dR}^2 \right] dR \tag{4.54}$$

or

$$\bar{V} = \pi [I_{b1}+I_{b2}+I_{b3}] + 12\pi [I_{m1}+I_{m2}+I_{m3}+I_{m4}+I_{m5}+I_{m6}] \tag{4.55}$$

where, for $b>1$ and $b\neq 2$,

$$I_{b1} = \int_0^1 R \frac{d^2W}{dR^2}^2 \, dR \tag{4.56}$$

$$I_{b2} = \int_0^1 \frac{1}{R} \frac{dW}{dR}^2 \, dR \tag{4.57}$$

$$I_{b3} = \int_0^1 2\mu \frac{dW}{dR} \frac{d^2W}{dR^2} \, dR \tag{4.58}$$

$$I_{m1} = \int_0^1 R \left(\frac{dU}{dR}\right)^2 dR \tag{4.59}$$

$$I_{m2} = \int_0^1 R \frac{dU}{dR} \left(\frac{dW}{dR}\right)^2 dR \tag{4.60}$$

$$I_{m3} = \int_0^1 \frac{R}{4} \left(\frac{dW}{dR}\right)^4 dR \tag{4.61}$$

$$I_{m4} = \int_0^1 \frac{U^2}{R} \, dR \tag{4.62}$$

$$I_{m5} = \int_0^1 2\mu U \frac{dU}{dR} \, dR \tag{4.63}$$

and

$$I_{m6} = \int_0^1 \mu U \left(\frac{dW}{dR}\right)^2 dR \, . \tag{4.64}$$

Note that (4.52) is not the result of superposition (which is only valid for linear operators). Equation (4.52) takes this form because mixed terms $\bar{e}^{b}{}_{i}\bar{e}^{m}{}_{j}$ in equation (4.51) become even functions with respect to Z after integration and subsequently disappear when evaluated from Z = -1/2 to 1/2. Now substituting (4.5) and (4.33) into (4.56) through (4.64) yields, after integration,

$$I_{b1} = 2bA^2 \tag{4.65}$$

$$I_{b2} = \frac{2bA^2}{(b-1)} \tag{4.66}$$

$$I_{b3} = 0 \tag{4.67}$$

$$\begin{aligned} I_{m1} = \frac{A^4}{4(b-2)^4}\{ & \left[\frac{(b-1)^2}{b}\right]f_1^2 + \left[-\frac{(2b-1)^2}{3b}+2\frac{(b+1)}{(b+2)}-1\right]f_1 f_2 \\ & + \left[3\frac{(2b-1)}{(b+1)}+\frac{(-5b+2)}{2b}\right]f_1 f_3 + \left[\frac{(b+2)}{2}-2\frac{(b+1)}{(b+2)}\right]f_2^2 \\ & + \left[-6\frac{(b+1)}{(b+4)}+2\frac{(b+1)}{(b+2)}+\frac{1}{2}\right]f_2 f_3 + \left[\frac{1}{2}\right]f_3^2 \} \end{aligned} \tag{4.68}$$

$$\begin{aligned} I_{m2} = \frac{-2b^2A^4}{(b-2)^4}\{ & \left[\frac{(-13b+2)}{12b} + \frac{2}{(b+2)} + \frac{(2b-1)}{2(b+1)}\right] f_1 \\ & + \left[\frac{(11b+2)}{12b} - \frac{2}{(b+2)} - \frac{(b+1)}{(b+4)}\right] f_2 \\ & + \left[\frac{3}{2(b+1)} + \frac{(b-2)}{4b} - \frac{6}{(b+4)} + \frac{2}{(b+2)}\right] f_3 \} \end{aligned} \tag{4.69}$$

$$I_{m3} = \frac{4A^4b^3}{3(2b-1)(b+1)(b+4)} \tag{4.70}$$

$$I_{m4} = \frac{A^4}{4(b-2)^4}\{ [\frac{1}{2(2b-1)}+\frac{(b-2)}{2b}]f_1^2 + [\frac{(1-3b)}{3b}+\frac{2}{(b+2)}]f_1 f_2$$

$$+ [\frac{1}{(b+1)}+\frac{(b-2)}{2b}]f_1 f_3 + [\frac{1}{2(b+1)}-\frac{2}{(b+2)}+\frac{1}{2}]f_2^2$$

$$+ [\frac{-2}{(b+4)}+\frac{2}{(b+2)}-\frac{1}{2}]f_2 f_3 + [\frac{1}{6}]f_3^2 \} \qquad (4.71)$$

$$I_{m5} = 0 \qquad (4.72)$$

and

$$I_{m6} = \frac{-2b^2A^4\mu}{(b-2)^4}\{ [\frac{1}{2(2b-1)} - \frac{(3b+14)}{12b} + \frac{2}{(b+2)} + \frac{1}{2(b+1)}] f_1$$

$$+ [\frac{(3b+2)}{12b} + \frac{1}{(b+1)} - \frac{2}{(b+2)} - \frac{1}{(b+4)}] f_2$$

$$+ [\frac{1}{2(b+1)} - \frac{(b+6)}{12b} - \frac{2}{(b+4)} + \frac{2}{(b+2)}] f_3 \} \qquad (4.73)$$

where $b>1$ and $b\neq2$ to prevent division by zero.

Also, the central load can be determined by means of the principle of virtual work. That is,

$$\bar{P}dA = d\bar{V} \qquad (4.74)$$

or

$$\bar{P} = \frac{d\bar{V}}{dA} . \qquad (4.75)$$

But for constant a, h, E, and μ, composite function $\bar{V}$ can be written as

$$\bar{V} = \bar{V}(A, b(A)) \qquad (4.76)$$

so Equation (4.75) becomes

$$\bar{P} = \frac{\partial \bar{V}}{\partial A} + \frac{\partial \bar{V}}{\partial b}\frac{db}{dA} \ . \tag{4.77}$$

As shown in Figure 5.1, values resulting from the next section reveal that $1.3<b<2.0$ for deflections of the order of plate thickness h. Within this range, db/dA is small for all combinations of a, h, E, and μ within the limitations set by our original assumptions and, as suggested by Figure 5.2, $\partial\bar{V}/\partial b=0$ in the vicinity of the optimal value for b. Consequently,

$$\frac{\partial \bar{V}}{\partial b}\frac{db}{dA} << \frac{\partial \bar{V}}{\partial A} \tag{4.78}$$

and

$$\bar{P} = \frac{\partial \bar{V}}{\partial A} \ . \tag{4.79}$$

This derivative can be performed numerically or, alternatively, can be obtained analytically yielding an explicit expression for the central load. The analytical form will be given at the end of the next section where the results for parameter b can be used to create a simpler formula for load $\bar{P}$.

4.4 SOLUTION VIA RESIDUAL MINIMIZATION

Recall the equivalent form of the Von Karman equations given by (3.63) to (3.65):

$$\frac{d}{dR}\left[\frac{1}{R}\frac{d}{dR}\left(R\frac{dW}{dR}\right)\right] = \frac{\bar{P}}{2\pi R} + \bar{S}^m{}_r\frac{dW}{dR} \tag{4.80}$$

$$\frac{d}{dR}\left(R\bar{S}^m{}_r\right) - \bar{S}^m{}_t = 0 \tag{4.81}$$

$$R\frac{d}{dR}\left(\bar{S}^m{}_r+\bar{S}^m{}_t\right) + 6(1-\mu^2)\frac{dW}{dR}^2 = 0\ . \tag{4.82}$$

So far, only Equations (4.81) and (4.82) have been used in the derivation of expressions for displacement, strain, stress, and energy. Now (4.80) will be incorporated into the solution.

Parameter b can be determined by minimizing the residual X obtained by subtracting the right hand side of (4.80) from the left:

$$X = \frac{d}{dR}\left[\frac{1}{R}\frac{d}{dR}\left(R\frac{dW}{dR}\right)\right] - \bar{S}^m{}_r\frac{dW}{dR} - \frac{\bar{P}}{2\pi R}\ . \tag{4.83}$$

Or, substituting (4.5) and (4.34) into (4.83) and rearranging,

$$\begin{aligned} X = {} & \frac{-2KAb}{b-2}\left\{\left[\frac{b}{b-1}\right]R^{3b-3} - \left[\frac{8b}{b+2}+\frac{b}{b-1}\right]R^{2b-1} + \left[\frac{b^2}{2}+\frac{8b}{b+2}\right]R^{b+1}\right. \\ & \left. + \left[\frac{f_1-f_2+f_3}{\mu-1}\right]R^{b-1} - \left[\frac{b^2}{2}\right]R^3 - \left[\frac{f_1-f_2+f_3}{\mu-1}\right]R\right\} \\ & + 2b^2AR^{b-3} - \frac{\bar{P}}{2\pi R} \end{aligned} \tag{4.84}$$

where $\bar{P}=\bar{P}(b)$ is obtained from evaluating (4.79) analytically or numerically for each value of b.

In order to minimize this residual over [0,1] with respect to parameter b, X(R) must be mapped to a real number for each b considered. The functional used here is

$$F(X) = \int_{\epsilon}^{1} |X| \, dR \qquad (4.85)$$

where the lower limit of integration ϵ is small but greater than zero. Note that care must be exercised in evaluation of (4.85) since

$$\lim_{R \to 0} X = \infty \quad . \qquad (4.86)$$

If the exact solution W were known and substituted into (4.80), as R approached zero both sides of the differential equation would approach ∞ at the same rate and the residual X would equal zero. With an approximate form however, there is a small difference between the rates of approach to ∞ and this results in the singularity expressed by Equation (4.86).

For the minimization of F(X), the integration is performed numerically and the optimal value of b is determined with a single variable search [20]. This has been found to yield good results if ϵ is judiciously selected so that most of the domain is considered and $X(\epsilon)$

is of the same order of magnitude as X evaluated at $R>\epsilon$. Of course, the question may arise as to whether a better functional F for residual X could have been chosen. In fact, however, trials with other functionals have been performed and resulting values for b are practically identical to those reported.

Some generalizations regarding these results are as follows:

1) To a first approximation, b depends only on A and not on input parameters a, E, h, and μ. This is apparent from Figure 5.1.

2) For $A<5.0$, $1.3<b<2.0$.

3) The limit of b as A approaches zero is two. This confirms that the present solution approaches the linear form for small deflections. See Equation (4.9).

4) Linear and quadratic least squares fits to b versus A give the approximate empirical formula

$$b = \begin{cases} 2.0 - 0.12A & 0<A<1.0 \\ 2.035 - 0.171A + 0.0116A^2, & 1.0<A<5.0 \end{cases} \quad (4.87)$$

and this satisfies the previously mentioned requirement that $b>1$ and $b\neq 2$.

5) For load determination, a simplified scheme for parameter b can be used with a subsequent difference of less than 1% for $0<A<2.0$, 2% for $2.0<A<4.0$, and 5% for

$4.0<A<5.0$:

$$b = \begin{cases} 1.90, & 0<A\leq 1.0 \\ 1.70, & 1.0<A\leq 2.0 \\ 1.50, & 2.0<A<5.0 \end{cases} \tag{4.88}$$

However, this should only be used for load evaluation since P. in particular, appears insensitive to small changes in b.

Finally, recall from (4.79) that

$$\bar{P} = \frac{\partial \bar{V}}{\partial A} \tag{4.89}$$

where $\bar{V}$ is given by (4.55) and (4.65) through (4.73). Substituting (4.88) into (4.89) with double precision yields

$$\bar{P} = \begin{cases} (50.405)A + (14.789+16.522\mu-11.209\mu^2)A^3 & 0<A\leq 1 \\ (51.881)A + (14.356+17.486\mu-11.158\mu^2)A^3 & 1<A\leq 2 \\ (56.549)A + (13.612+16.002\mu-11.226\mu^2)A^3 & 2<A<5 \end{cases} \tag{4.90}$$

so that formulae now exist for all desired quantities and the original problem has been solved.

4.5 SUMMARY OF SOLUTION

The new solution for nonlinear deflection of point loaded clamped circular plates can be summarized thus:

$$W = \frac{A}{b-2}\left[2R^b - bR^2 + b - 2\right] \tag{4.91}$$

$$\bar{e}^b{}_r = \frac{-2bAZ}{b-2}\left[(b-1)R^{b-2} - 1\right] \tag{4.92}$$

$$\bar{e}^b{}_t = \frac{-2bAZ}{b-2}\left[R^{b-2} - 1\right] \tag{4.93}$$

$$\bar{S}^b{}_r = \frac{-24bAZ}{b-2}\left[(b-1+\mu)R^{b-2} - 1 - \mu\right] \tag{4.94}$$

$$\bar{S}^b{}_t = \frac{-24bAZ}{b-2}\left[(\mu b-\mu+1)R^{b-2} - 1 - \mu\right] \tag{4.95}$$

$$U = \frac{K}{12(1-\mu^2)}\left[f_1R^{2b-1} - f_2R^{b+1} + f_3R^3 - f_1R + f_2R - f_3R\right] \tag{4.96}$$

$$\bar{e}^m{}_r = \frac{K}{12(1-\mu^2)}\left[\frac{b(-2\mu b+\mu+1)}{b-1}R^{2b-2} - \frac{8b(-\mu b-\mu+1)}{b+2}R^b + \frac{b^2(1-3\mu)}{2}R^2 - f_1 + f_2 - f_3\right] \tag{4.97}$$

$$\bar{e}^m{}_t = \frac{K}{12(1-\mu^2)}\left[f_1R^{2b-2} - f_2R^b + f_3R^2 - f_1 + f_2 - f_3\right] \tag{4.98}$$

$$\bar{S}^{m}_{r} = K\left[\frac{bR^{2b-2}}{b-1} - \frac{8bR^{b}}{b+2} + \frac{b^{2}R^{2}}{2} + \frac{f_1-f_2+f_3}{\mu-1}\right] \tag{4.99}$$

$$\bar{S}^{m}_{t} = K\left[\frac{b(2b-1)R^{2b-2}}{b-1} - \frac{8b(b+1)R^{b}}{b+2} + \frac{3b^{2}R^{2}}{2} + \frac{f_1-f_2+f_3}{\mu-1}\right] \tag{4.100}$$

$$\bar{P} = \begin{cases} (50.405)A + (14.789+16.522\mu-11.209\mu^{2})A^{3} & 0<A\leq 1 \\ (51.881)A + (14.356+17.486\mu-11.158\mu^{2})A^{3} & 1<A\leq 2 \\ (56.549)A + (13.612+16.002\mu-11.226\mu^{2})A^{3} & 2<A<5 \end{cases} \tag{4.101}$$

where

$$K = \frac{-6(1-\mu^{2})A^{2}}{(b-2)^{2}} \tag{4.102}$$

$$f_1 = \frac{b(2b-1-\mu)}{b-1} \tag{4.103}$$

$$f_2 = \frac{8b(b-\mu+1)}{b+2} \tag{4.104}$$

$$f_3 = \frac{b^{2}(3-\mu)}{2} \tag{4.105}$$

and

$$b = \begin{cases} 2.0 - 0.12A & 0<A<1.0 \\ 2.035 - 0.171A + 0.0116A^{2}, & 1.0<A<5.0 \end{cases} \tag{4.106}$$

These expressions satisfy the criterion of generality and a discussion of the accuracy, range of applicability, and

usefulness of this solution will be presented Chapter 5.

CHAPTER 5

RESULTS AND DISCUSSION

The behaviour of a point loaded circular plate and the fundamental characteristics of the new solution, in particular, can be obtained by interpreting Figures 5.1 to 5.22. For example, Figures 5.2 and 5.3 show that residual rather than energy minimization is necessary since plots of energy versus parameter b are nearly flat in the regions of interest and do not indicate one definite minimum. In addition, the nature of displacements, stresses, and load-deflection relationships is revealed in Figures 5.4 to 5.22 where the present solution is compared to the results of Brodland, Volmir, Schmidt, Basuli, and Chien and Yeh. Unless otherwise indicated, all curves are for D=1000, h=0.1, and a=10. Also, Volmir's and Schmidt's results are given for a Poisson's ratio of 0.3 while those of Brodland and Chien and Yeh are for μ=0.5. Unfortunately, more than one value of Poisson's ratio must be used in these comparisons since Schmidt's published results are strictly valid for only μ=0.3, and Brodland's numerical scheme is applicable only to incompressible materials. Note, however, that Volmir's load-deflection curve for μ=0.3 in Figure 5.8 does compare very well to those for μ=0.5 since the flexural rigidity D is the same, and, of the three dimensionless parameters describing the present problem,

Poisson's ratio has the weakest influence [2]. The effect of μ is mainly seen in the remaining figures where, in general, two distinct groups of curves are evident.

Examination of the transverse deflection profiles in Figures 5.4 and 5.5 reveals that as displacements increase, the shape of the plate does in fact change and only Volmir's linear model retains its original small deflection shape. Also, radial displacements are given in Figures 5.6 and 5.7 where u is noted to change sign over $0 \leq R \leq 1$. The nature of geometric nonlinearity is illustrated by the load-deflection curves of Figure 5.8 in conjunction with Figures 5.17 to 5.22 which show that the plate becomes more rigid with increasing deflection as membrane effects supplement bending effects. Finally, the trends in Figures 5.9 to 5.16 show that the membrane stress as well as the extreme fiber bending stress is greatest at the center of the plate and, in fact, all solutions except for the numerical results of Brodland exhibit a singularity in the bending stress functions at R=0 where $S^b{}_r$ and $S^b{}_t$ approach infinity.

The absolute accuracy of the present approach cannot be estimated for there is not yet an exact solution to serve as a basis for comparison. That is, we can only check for agreement with other approximate solutions. Of these, Brodland's results should be considered most carefully since his numerical scheme has proven accurate for the analysis of other thin shell problems and is valid for

center deflections up to ten times the plate's thickness.

In general, Figures 5.4 to 5.22 indicate that the analytical solutions compare well with Brodland's algorithm with certain notable exceptions. For example, in Figures 5.19 and 5.20, Chien and Yeh's curves for membrane stress at the edge of the plate diverge badly for $\bar{P}$ greater than 300 and this type of occurrence is not evident in any other Chien and Yeh results. A possible explanation for this phenomenon may be proposed by considering the nature of this perturbation solution. Only two terms of the series are published and accuracy therefore depends on the rate and type of convergence. That is, if the series does not converge uniformly, the truncated expression might be accurate for only a portion of the domain as in these figures.

A second instance of relatively poor agreement can be found in Figures 5.17 and 5.18 where bending stresses at R=1 differ considerably for $\bar{P}>100$. Although it is not certain which curves are in error, it can be noted that for the present 'assumed form' solution, determination of bending stress is far less rigorous than the corresponding derivation of membrane stress. In fact, $S^b{}_r$ and $S^b{}_t$ are obtained simply by substituting the displacement model W directly into the strain-displacement relations which are, in turn, substituted into the constitutive equations. Consequently, the influence of the Von Karman equations is represented only by the value of constant b and the

accuracy of the resulting expressions is much more sensitive to any error in this parameter. Also, the validity of assuming the bending stress to be symmetric about the middle surface of the plate comes into question as transverse deflections become very large. Therefore, this might lead one to expect that the curves for membrane stress are more accurate than those for bending.

Additional anomalies can be seen in Figures 5.5, 5.8 and 5.19. In Figure 5.8, Schmidt's load-deflection relation is noticeably different from the others for central normalized deflections greater than 3.0, while in Figure 5.19, his curve for radial membrane stress at the edge deviates for dimensionless loads $\bar{P}$ greater than 400. In Figure 5.5, the transverse deflection profiles generated by the solutions of Volmir, Basuli and Chien and Yeh are considerably different from those produced by Dolovich and Brodland for A=3.0. If we accept Brodland's results as the basis for comparison, Figure 5.5 suggests that the new nonlinear displacement model constitutes an improvement over previous expressions for describing the nature of large plate deflections.

Except for the cases just described, the present approach as well as solutions by Brodland, Volmir, Schmidt, Chien and Yeh, and Basuli seem to give comparable quantitative results over a deflection range of up to five times plate thickness h. However, Schmidt does not give general expressions for stress and displacement while

Basuli derives displacement equations which are difficult to use. As a result, only Volmir and Chien and Yeh present analytical formulas which rival those of the new solution.

The contribution provided here, is the confirmation of previously determined characteristics and the revelation of unidentified aspects of the plate's behaviour. The latter accomplishment is chiefly due to the analysis of our starting point, displacement model W. For example, in Chapter 4 we remarked that this model approaches the Lagrange lateral displacement solution for decreasing w_o/h and, subsequently, we produced an expression for R_c, the inflection point of the plate:

$$R_c = (b-1)^{1/(2-b)} . \qquad (4.10)$$

We now note that

$$\lim_{b \to 1} R_c = 0 \qquad (5.1)$$

and this is of interest since, in general, w_o/h increases for decreasing b, and as a plate's response approaches that of a membrane, its point of inflection should move towards the center until, in the limit, it is located at R=0. So, future examination of possible ramifications of b=1 in the solution development given in Chapter 4 might shed light on the behaviour of point loaded membranes.

In addition, the aforementioned confirmation of previously determined characteristics is not restricted to the curves given in Figures 5.4 to 5.22. Reexamination of Equation (4.101) reveals that this simplified expression

for the central load is identical in form to that produced by series methods even though it has been obtained in a completely different way. Specifically, for $\mu=0.3$, and $0<A<1.0$ Schmidt and Chien and Yeh give respectively:

$$\bar{P}_S = 50.27\ A + 22.36\ A^3 - 1.21\ A^5 + 0.22\ A^7 \tag{5.2}$$

$$\bar{P}_{CY} = 16\pi A + 22.36\ A^3 \tag{5.3}$$

while from (4.101),

$$\bar{P} = \begin{cases} 50.41\ A + 18.74\ A^3 & 0<A\leq 1.0 \\ 51.88\ A + 18.60\ A^3 & 1.0<A\leq 2.0 \\ 56.55\ A + 17.40\ A^3 & 2.0<A<5.0 \end{cases} \tag{5.4}$$

In each case, the two first terms take the form

$$\bar{P} = k_1 A + k_2 A^3 \tag{5.5}$$

where even powers of A are not included and k_1 and k_2 are constants. Also, the first term in each expression is equal or approximately equal to the corresponding linear result

$$\bar{P} = 16\pi\ A\ . \tag{5.6}$$

On the other hand, for $0<A<1.0$ constant k_2 in (5.4) differs by about 16 percent from its value in (5.2) and (5.3). However, as seen in Figure 5.8 a significant disparity in the load-deflection curves is not evident until center normalized deflections are fairly large.

Thus, the new displacement model presented generates

some interesting solution characteristics. However, before concluding, it must be made clear that not all properties of point loaded plates have been herein discussed. There are certain issues which constitute detailed subjects in themselves and therefore are only mentioned.

For example, discussion of the various implications of a point load can take a direction that requires reevaluation of the most basic of assumptions. Physically, there is no such thing as a true point load; that is, a force acting over an infinitely small area. Therefore, we must classify the point load as part of the mathematical problem which consists of the Von Karman equations and clamped boundary conditions and which serves to model the effect of central loads applied over areas of relatively small radius. Even the mathematical solution must be regarded with caution since, by definition, the stress at the point of application of load P on the surface is infinitely large and results should be viewed in light of St. Venant's principle [7].

However, we can say that the solution presented is of practical usefulness and compares well with expressions for stress, strain, load, and deflection obtained by other means. It is very general and the introduction of the nonlinear displacement model provides new insight into the large deflection of a point loaded circular plate.

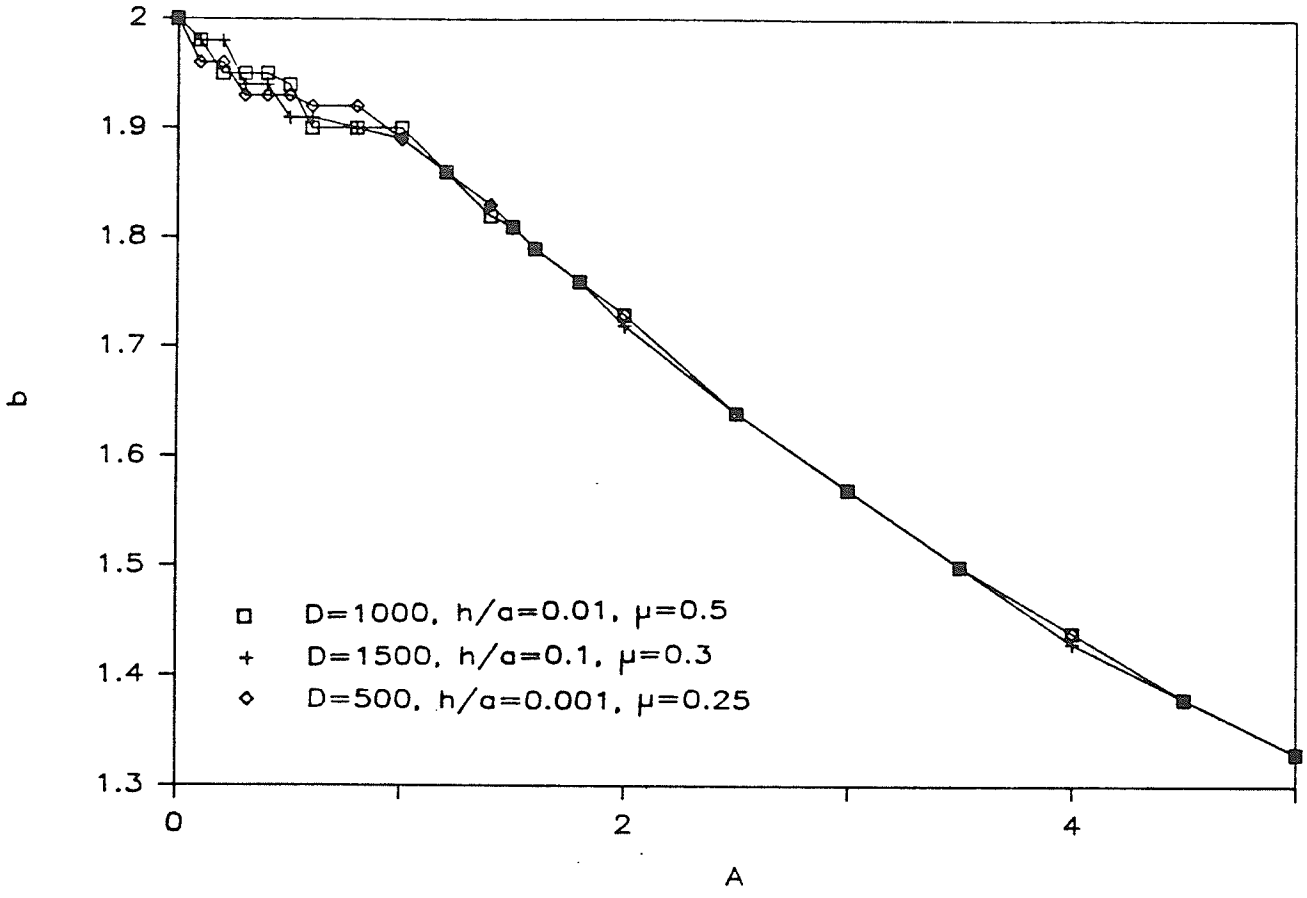

Figure 5.1 Sensitivity of b to Input Parameters

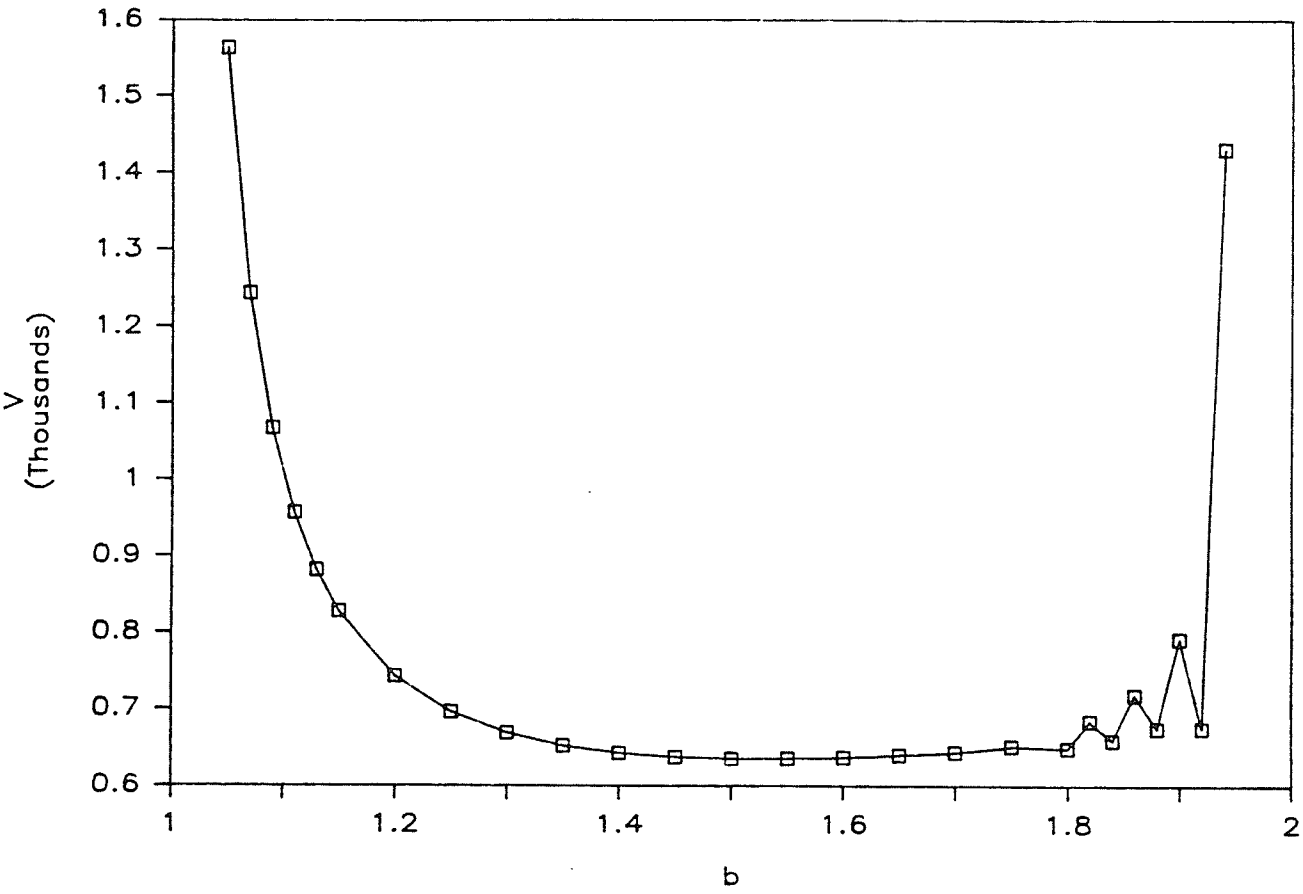

Figure 5.2 Strain Energy Versus Parameter b for A=3.0

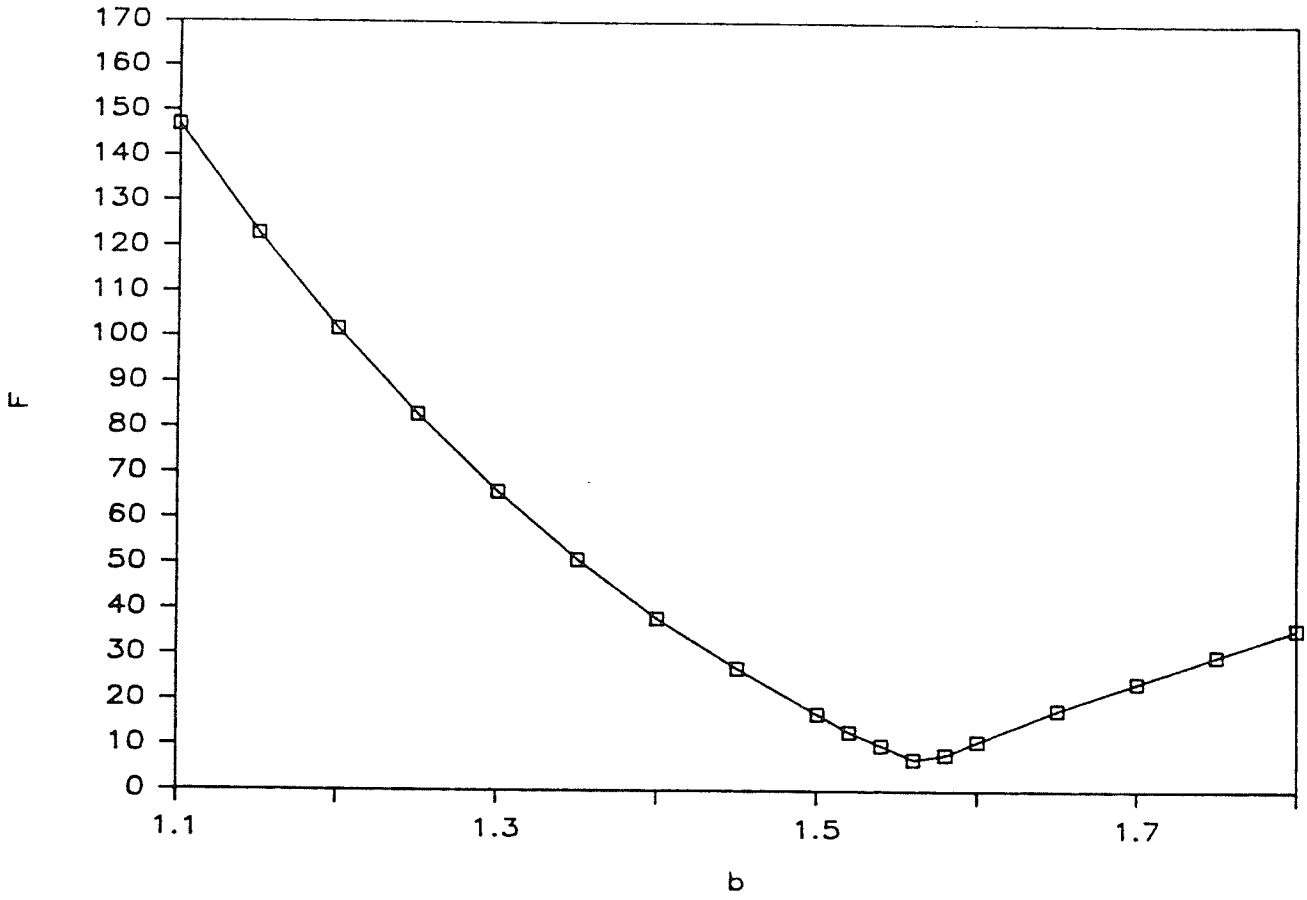

Figure 5.3 Functional F Versus Parameter b for A=3.0

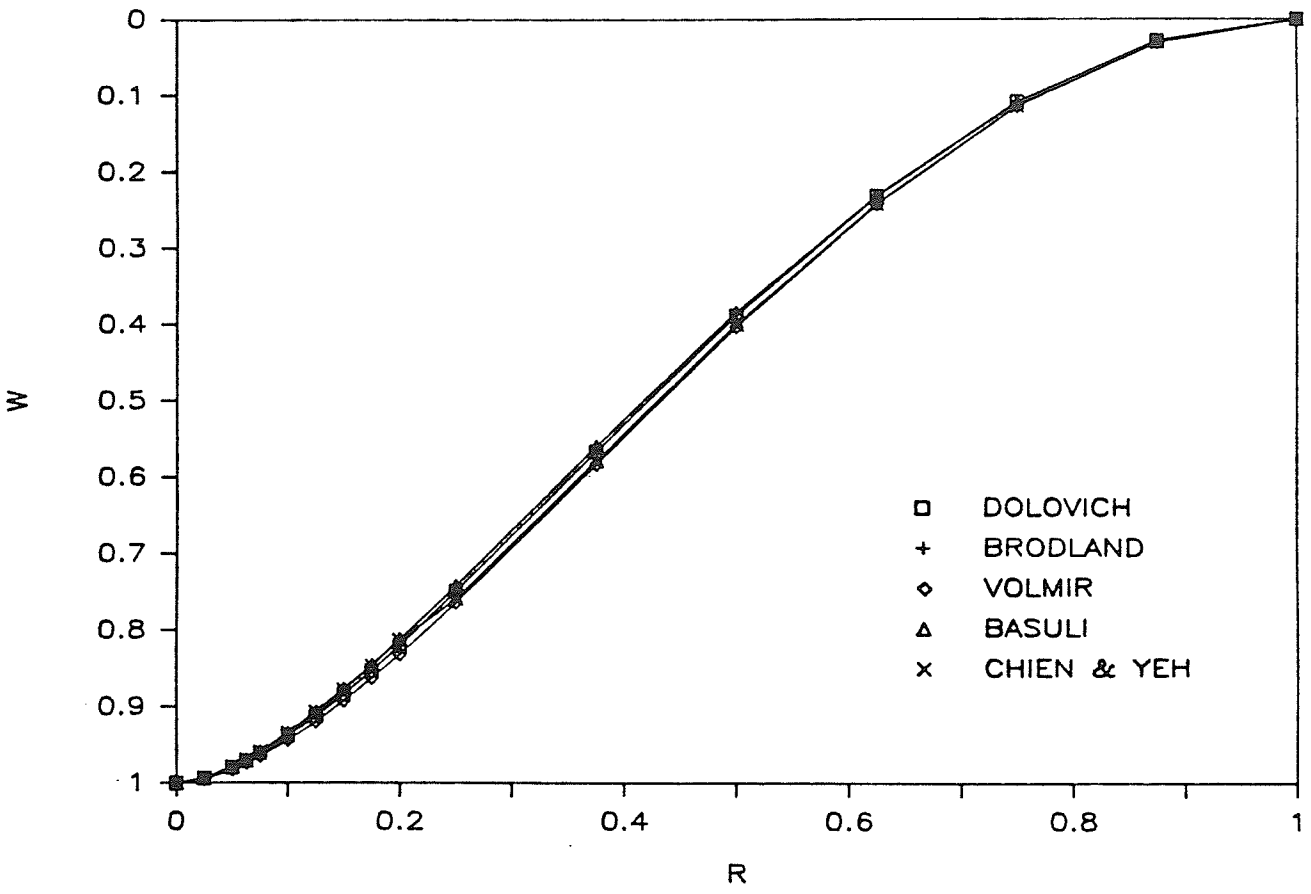

Figure 5.4 Transverse Deflection Profile for A=1.0

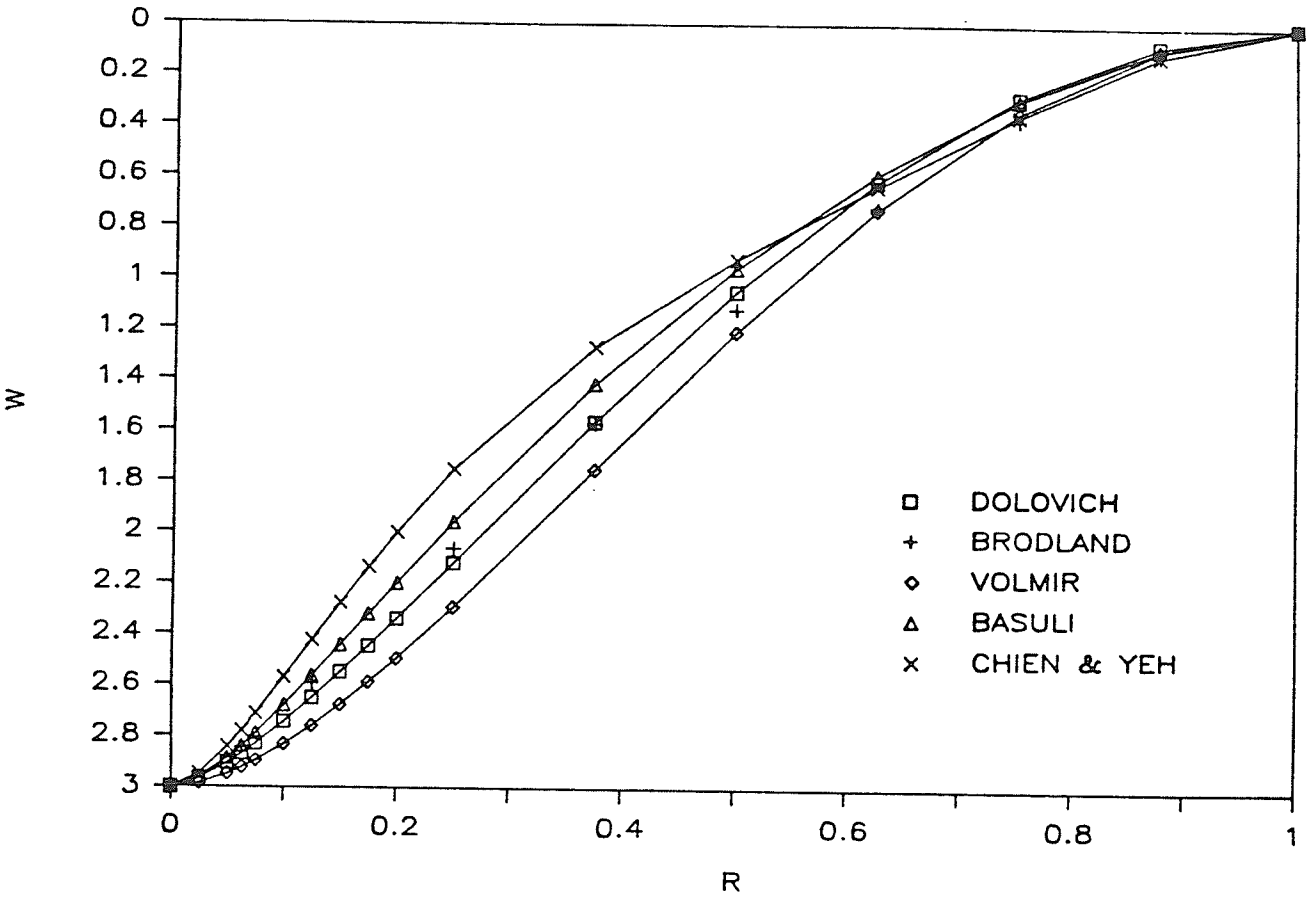

Figure 5.5 Transverse Deflection Profile for A=3.0

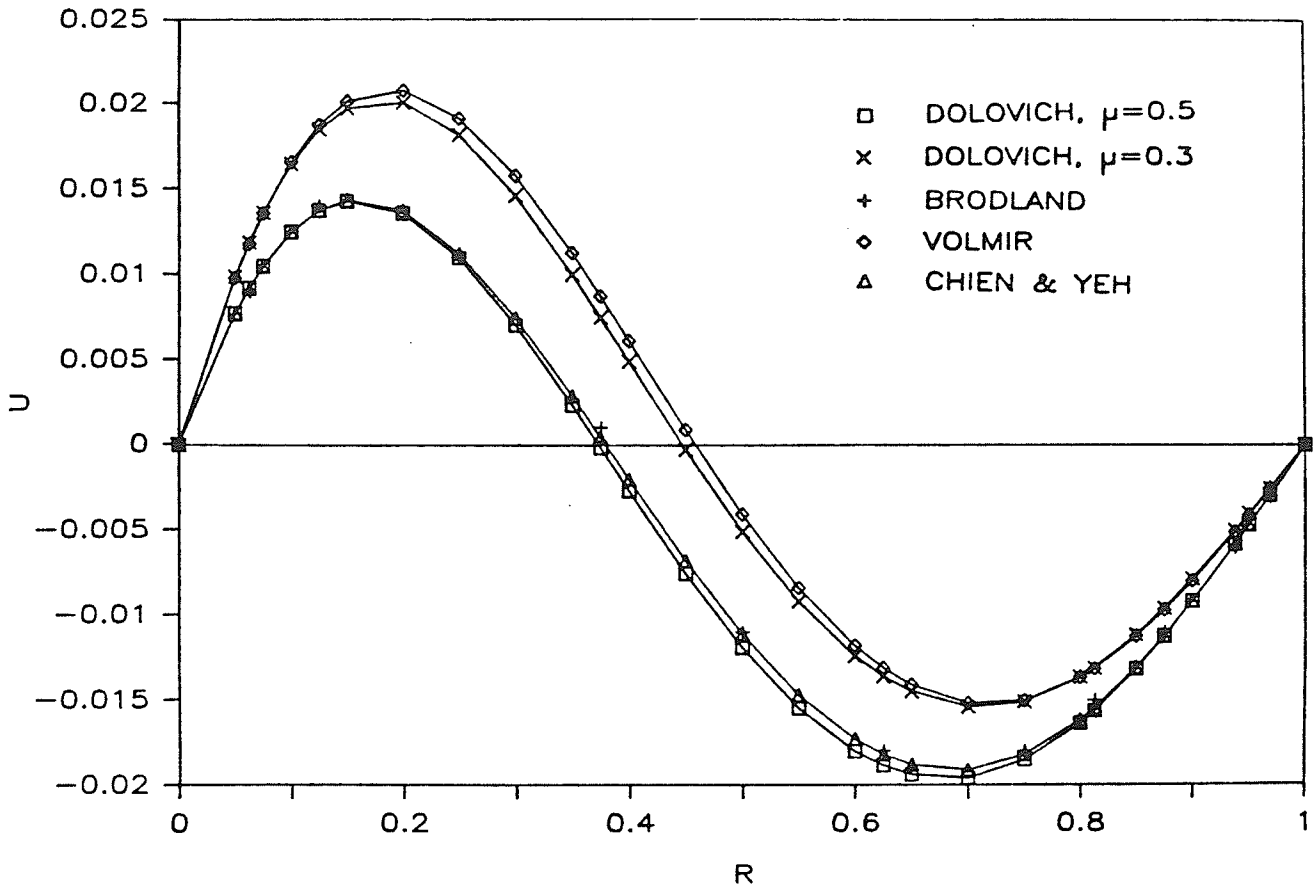

Figure 5.6 Radial Deflection Profile for A=0.5

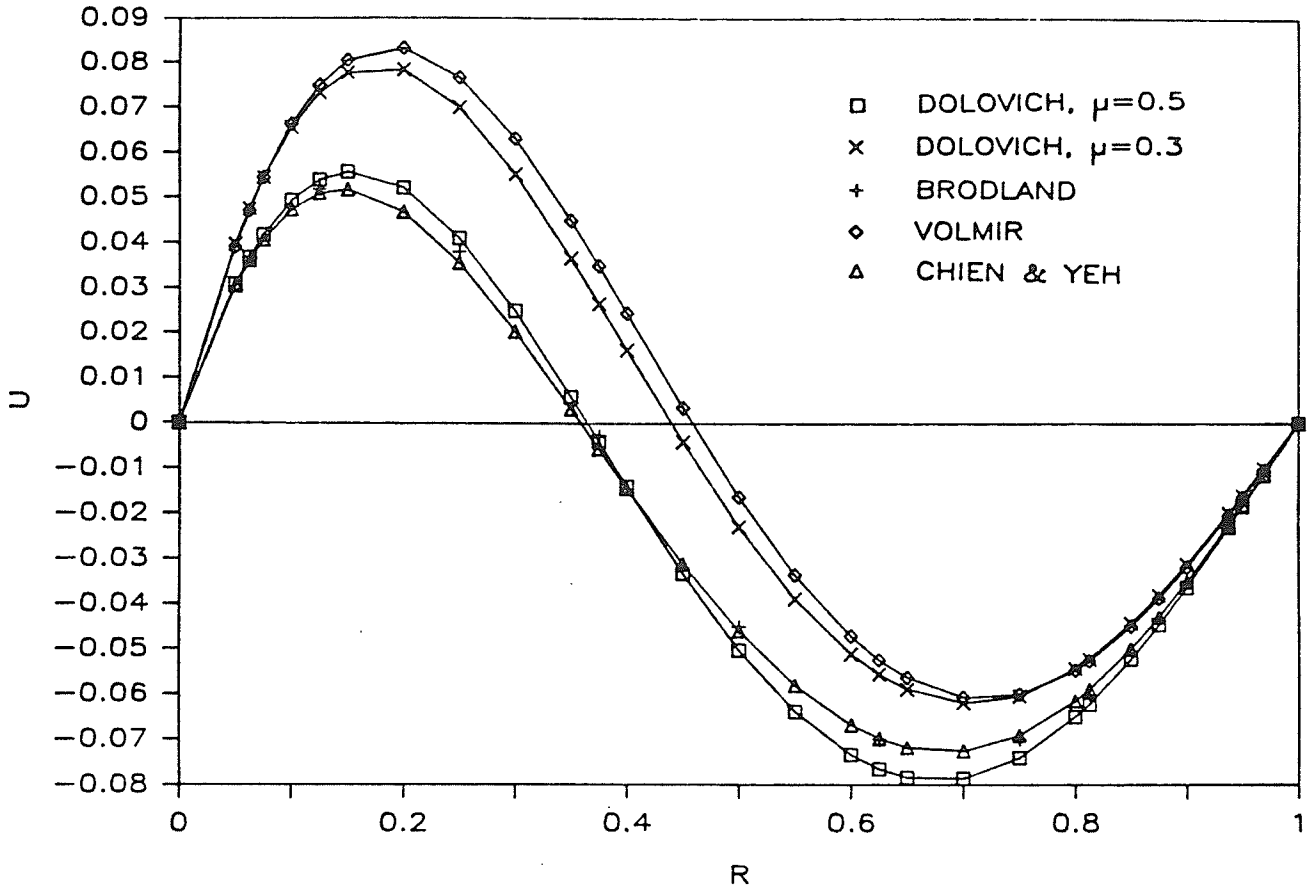

Figure 5.7 Radial Deflection Profile for A=1.0

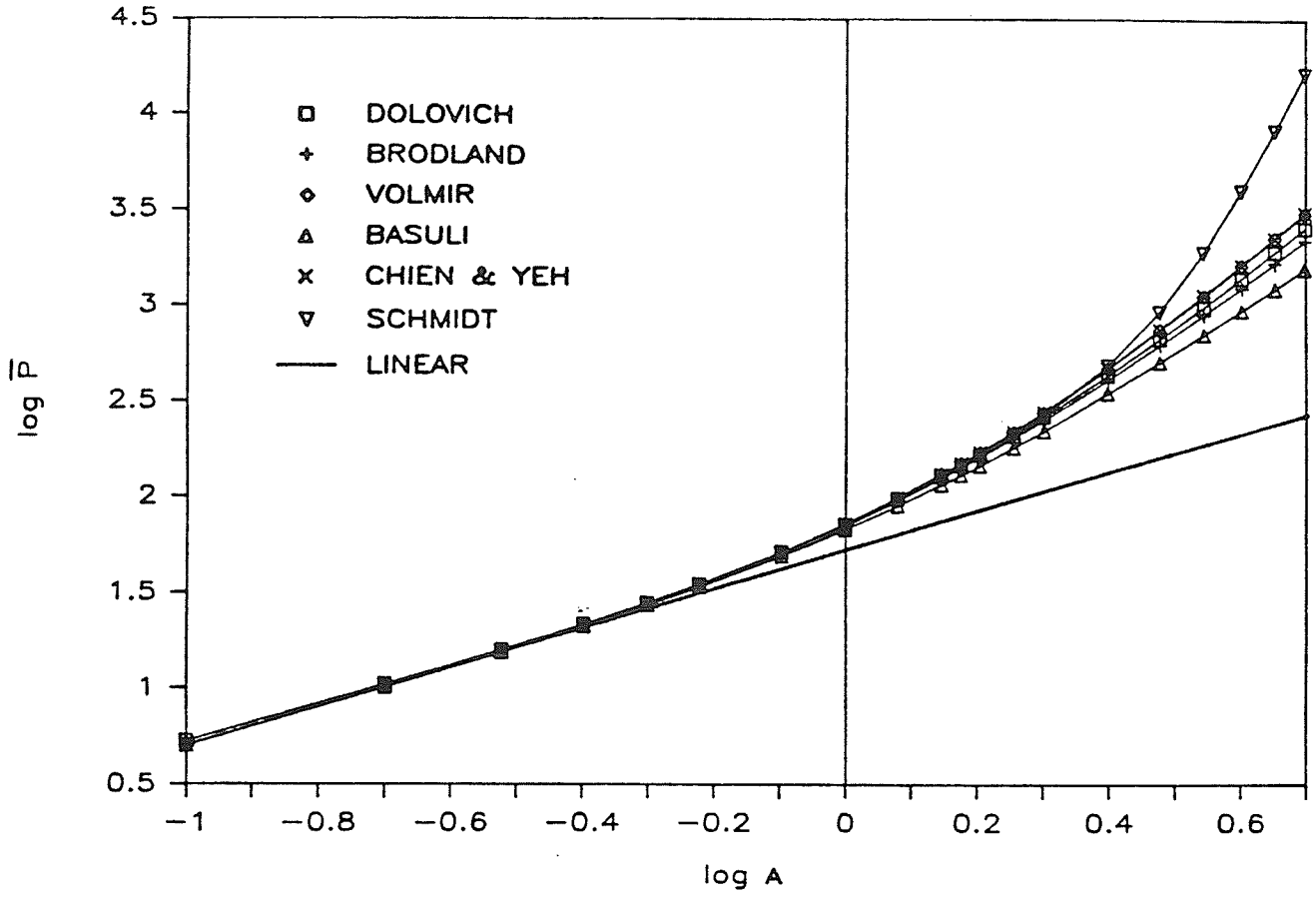

Figure 5.8 Load Versus Center Deflection

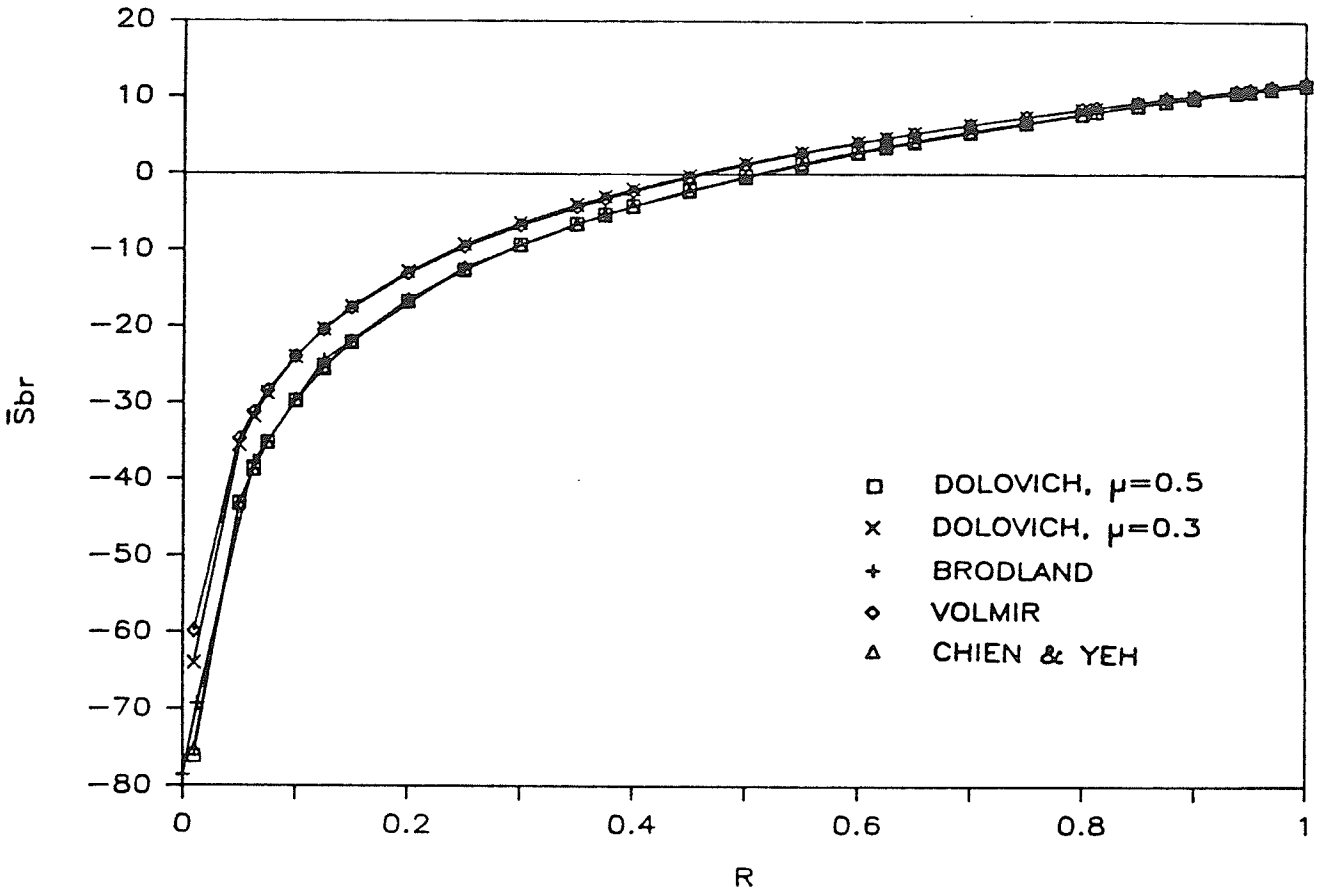

Figure 5.9 Radial Bending Stress Profiles for A=0.5

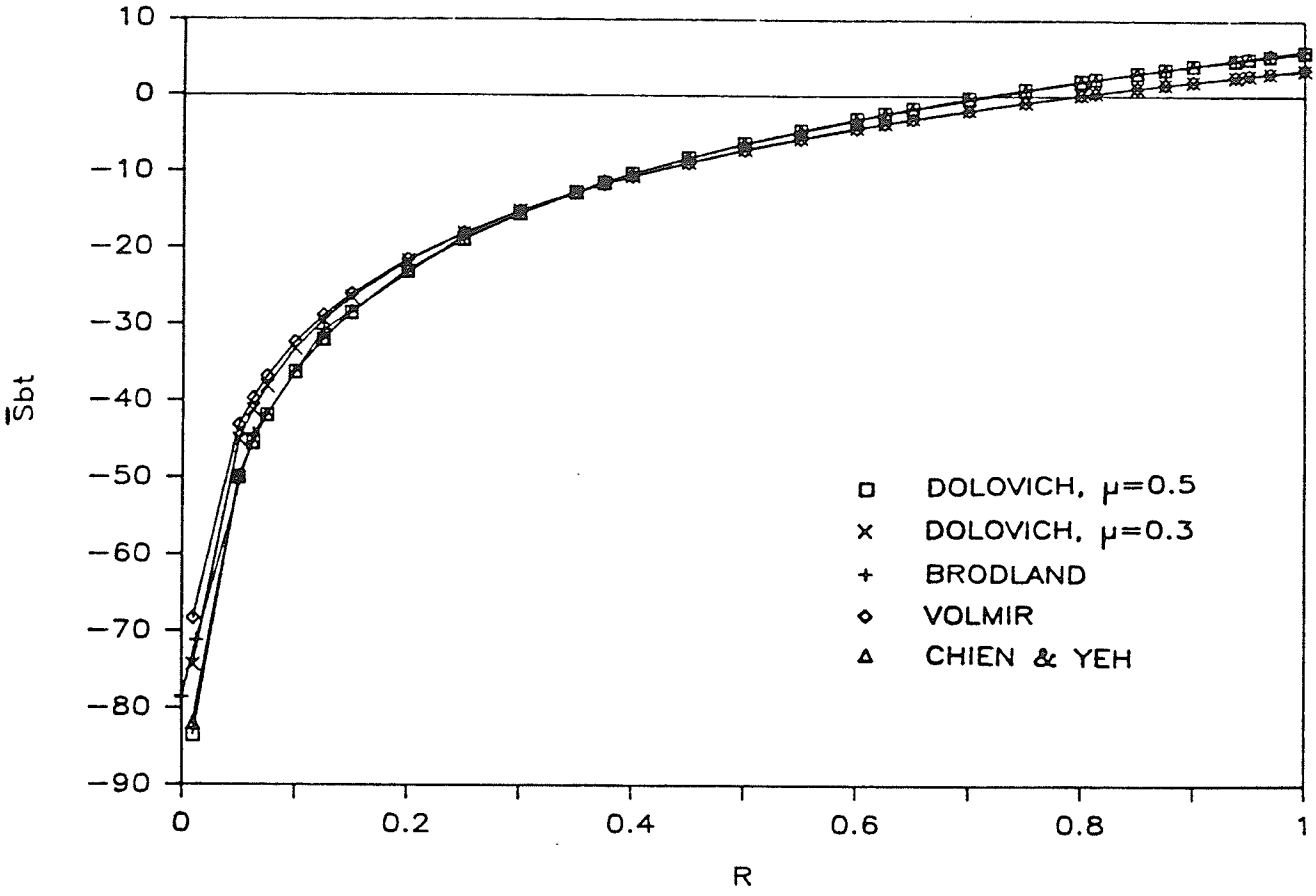

Figure 5.10 Tangential Bending Stress Profiles for A=0.5

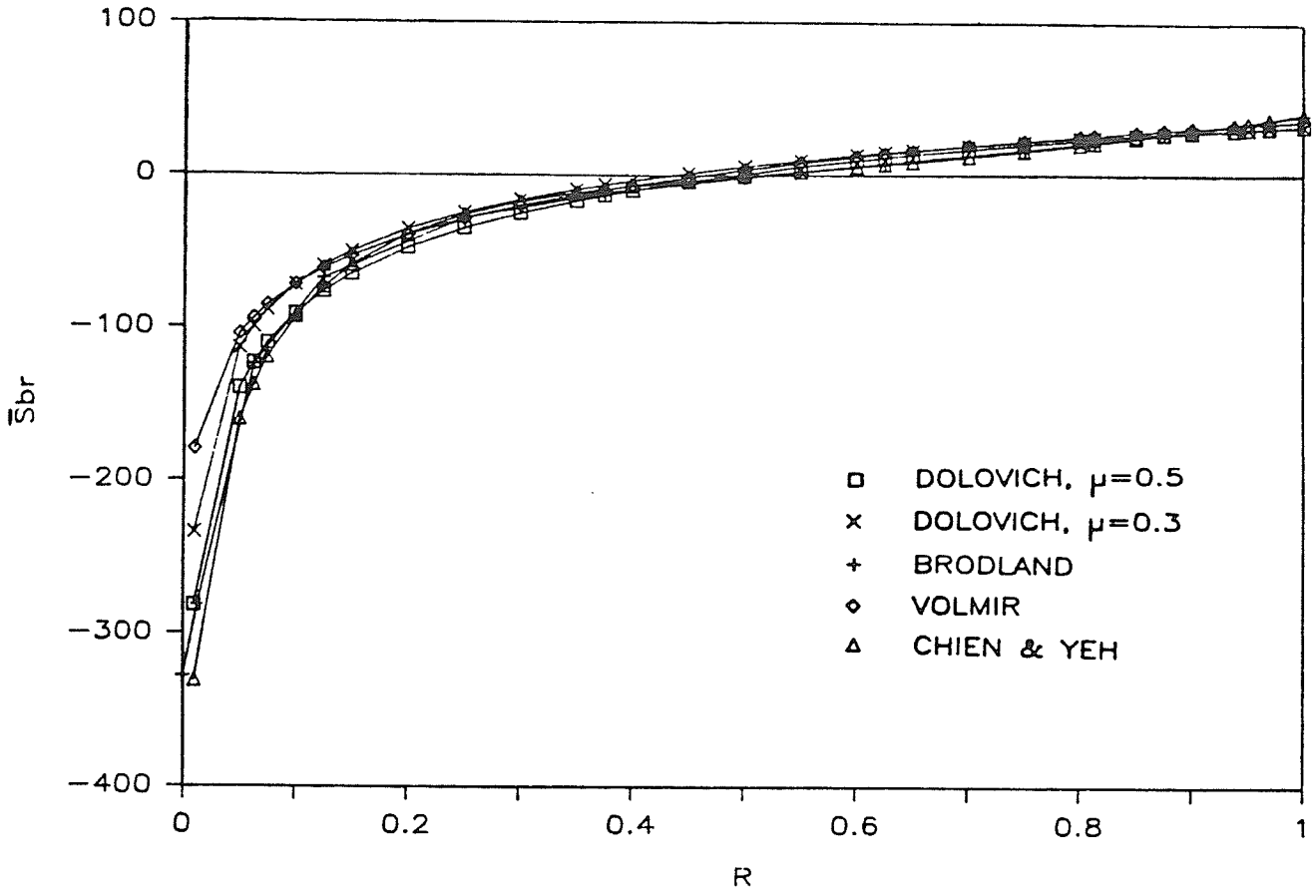

Figure 5.11 Radial Bending Stress Profiles for A=1.5

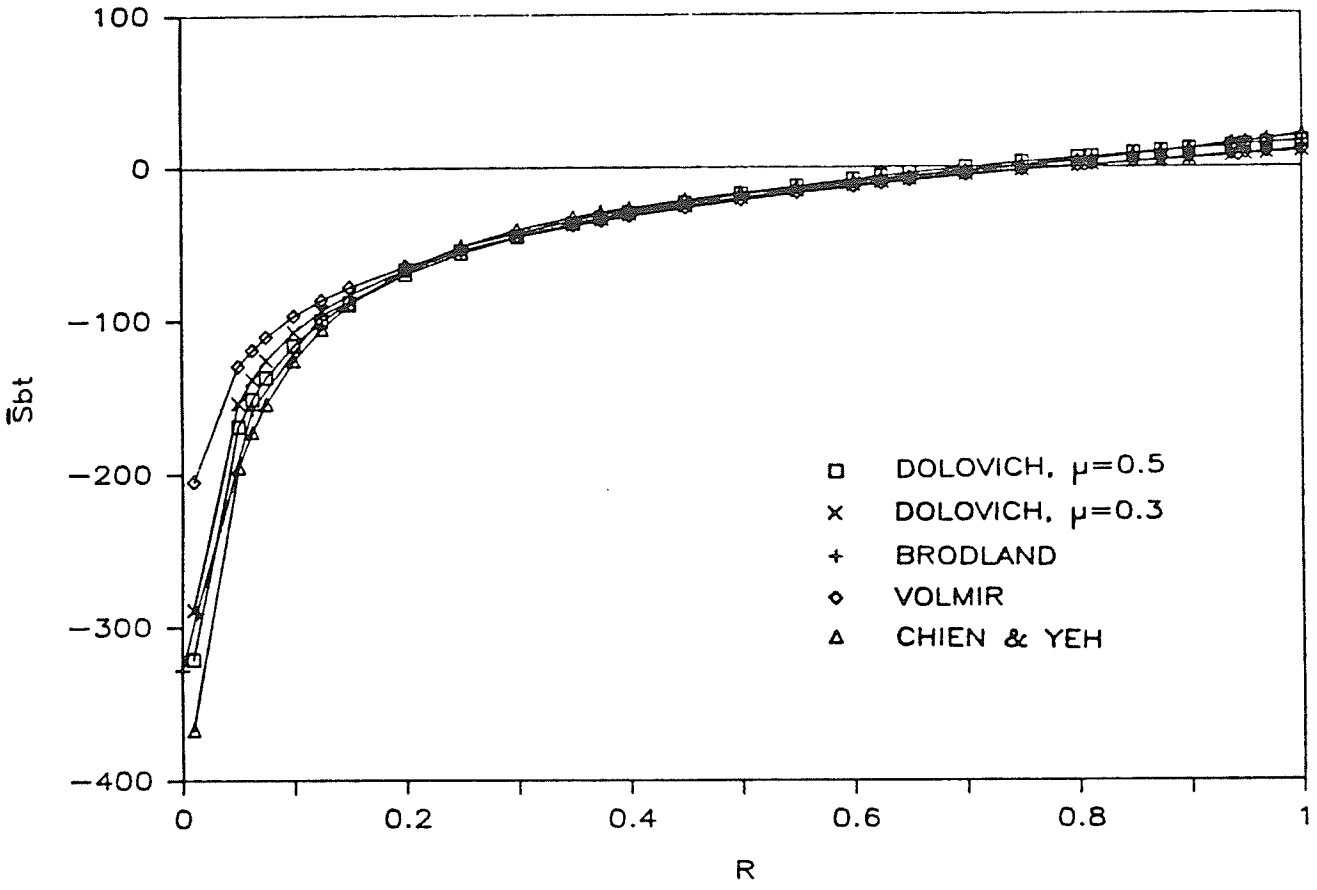

Figure 5.12 Tangential Bending Stress Profiles for A=1.5

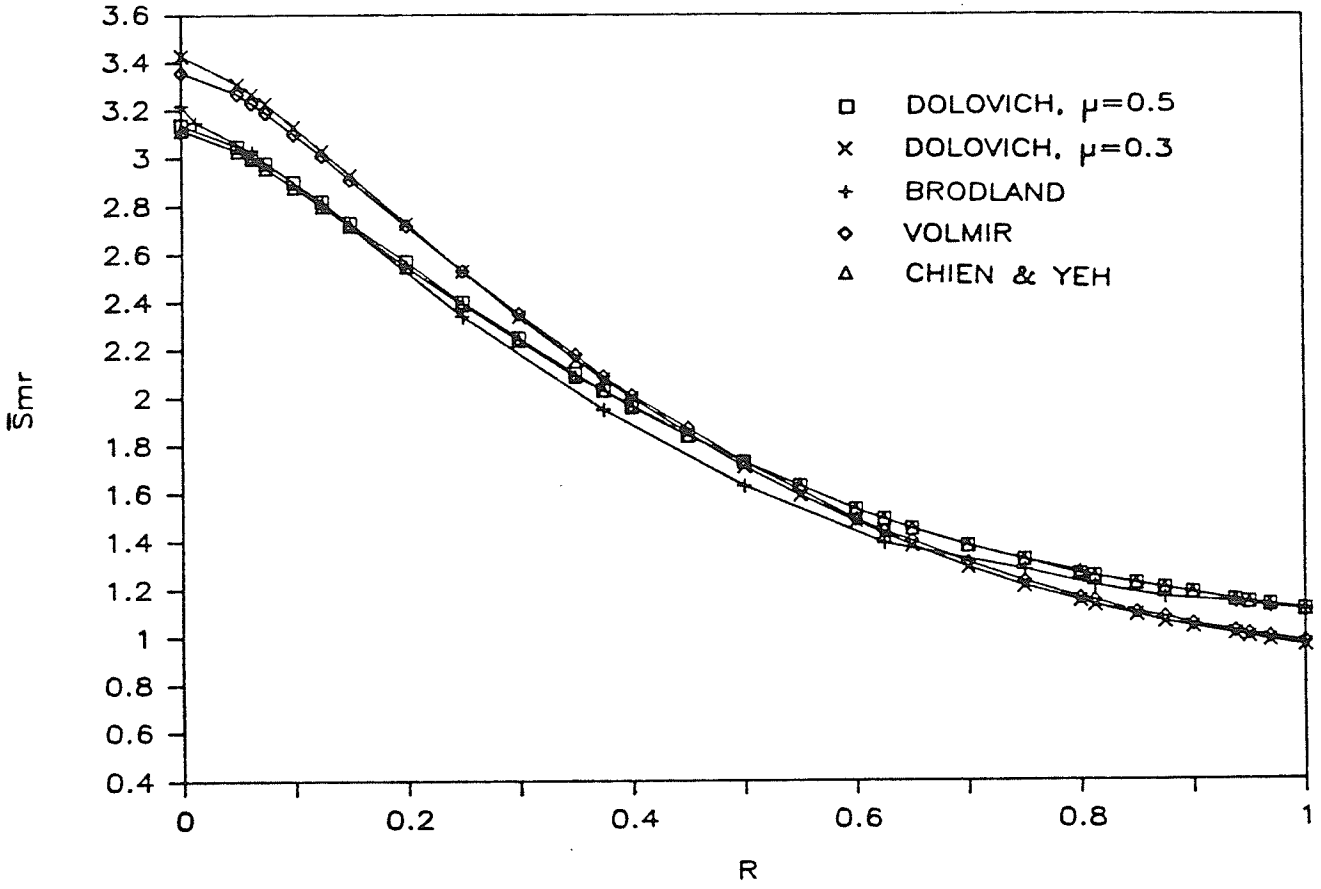

Figure 5.13 Radial Membrane Stress Profiles for A=0.5

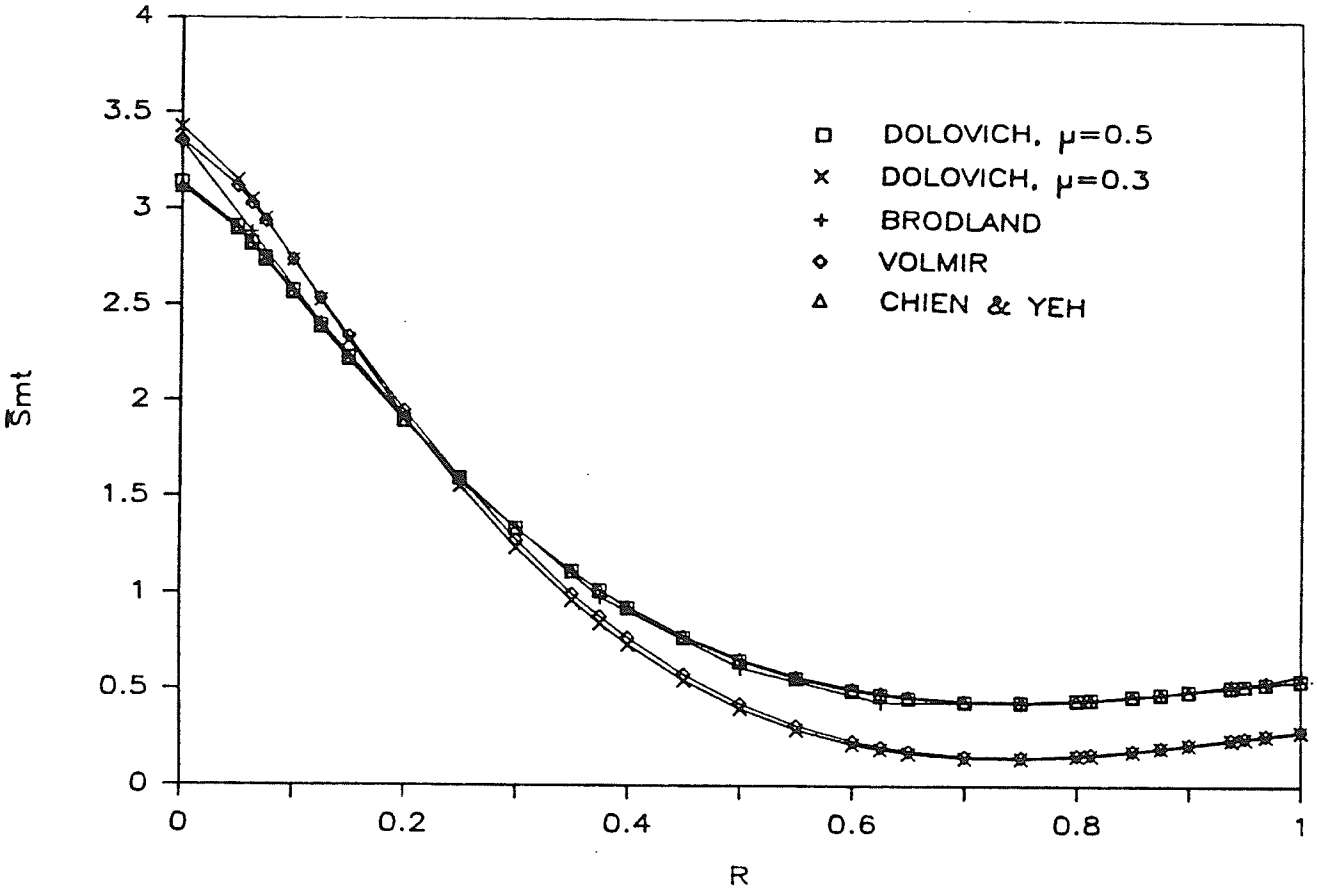

Figure 5.14 Tangential Membrane Stress Profiles for A=0.5

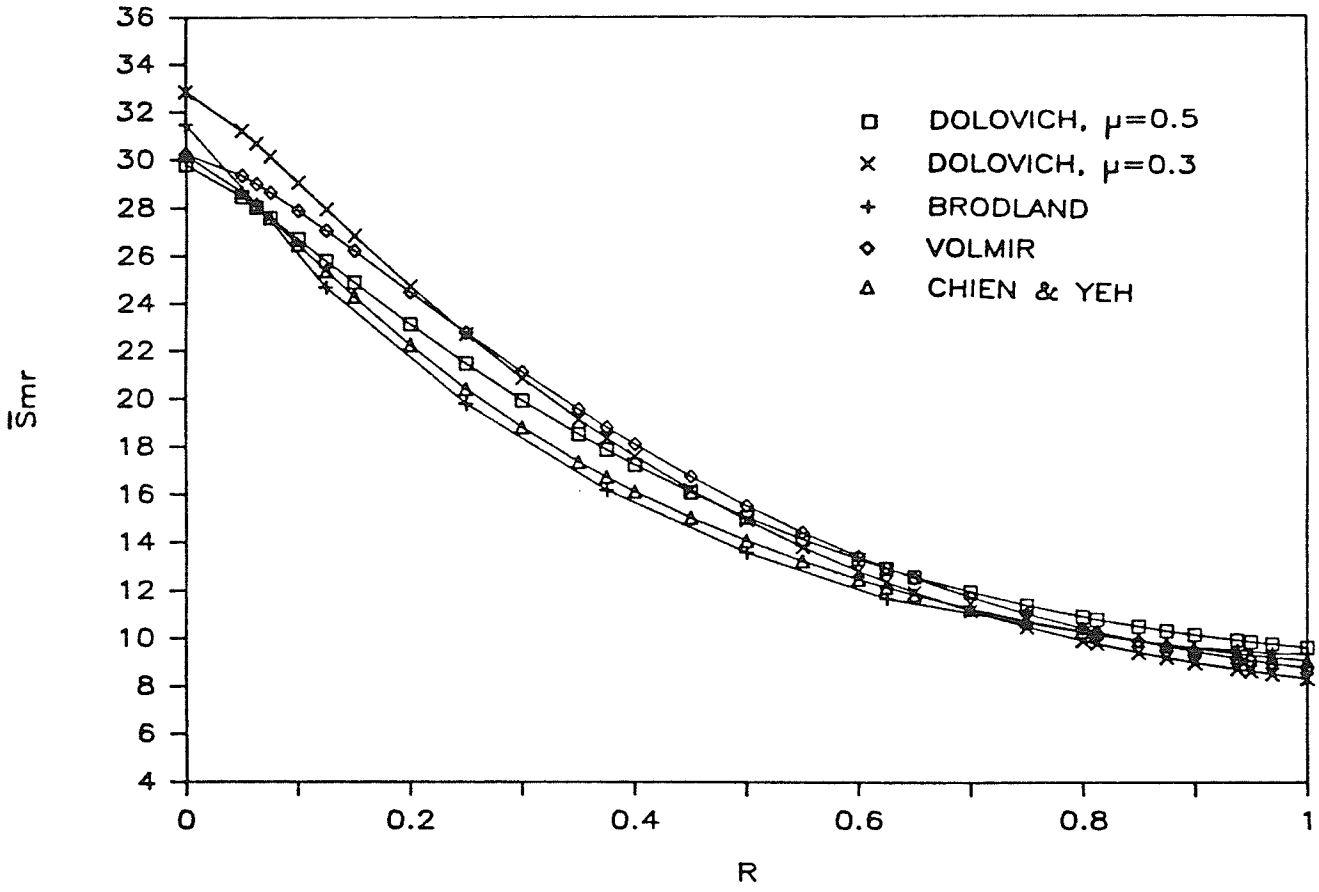

Figure 5.15 Radial Membrane Stress Profiles for A=1.5

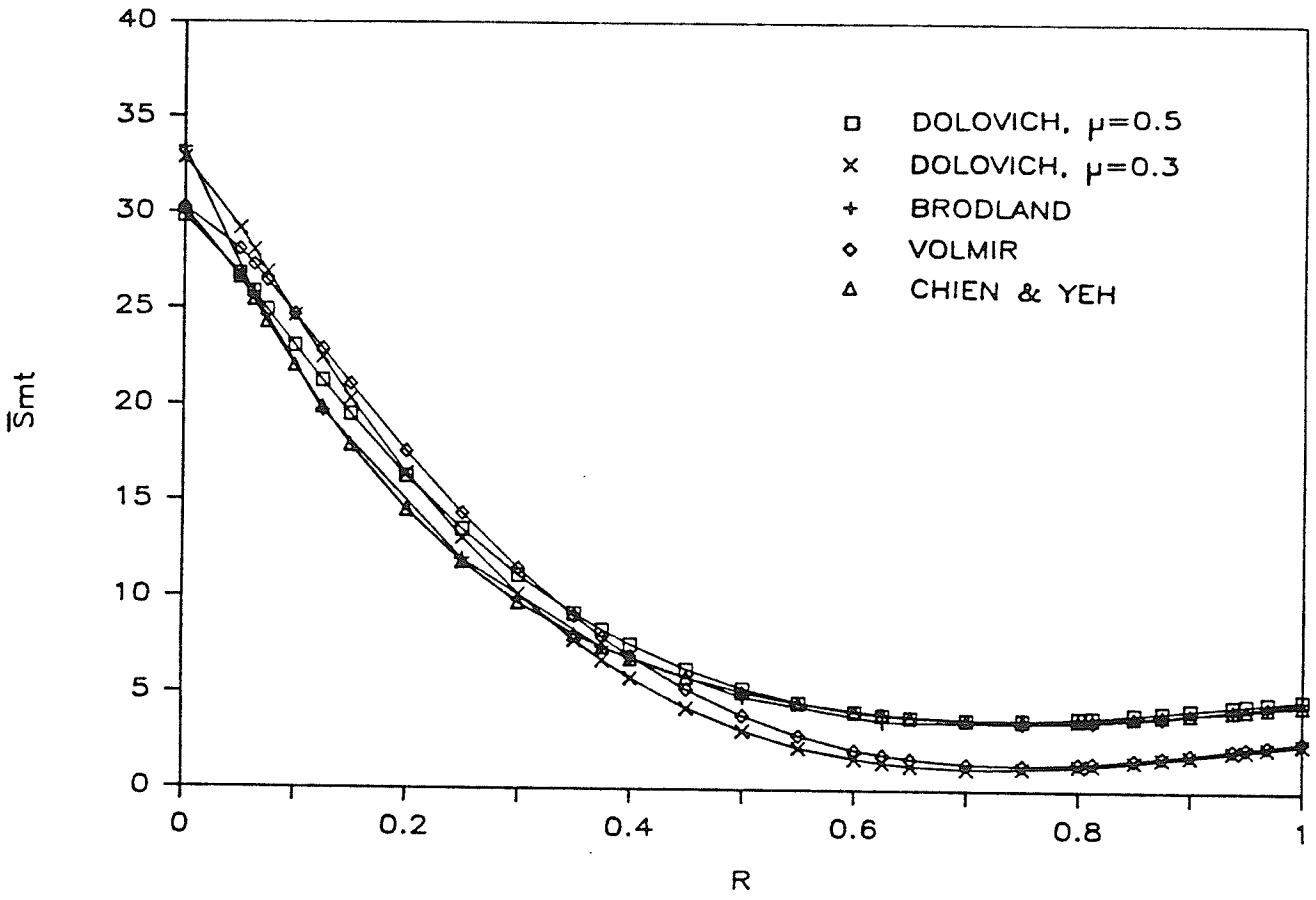

Figure 5.16 Tangential Membrane Stress Profiles for A=1.5

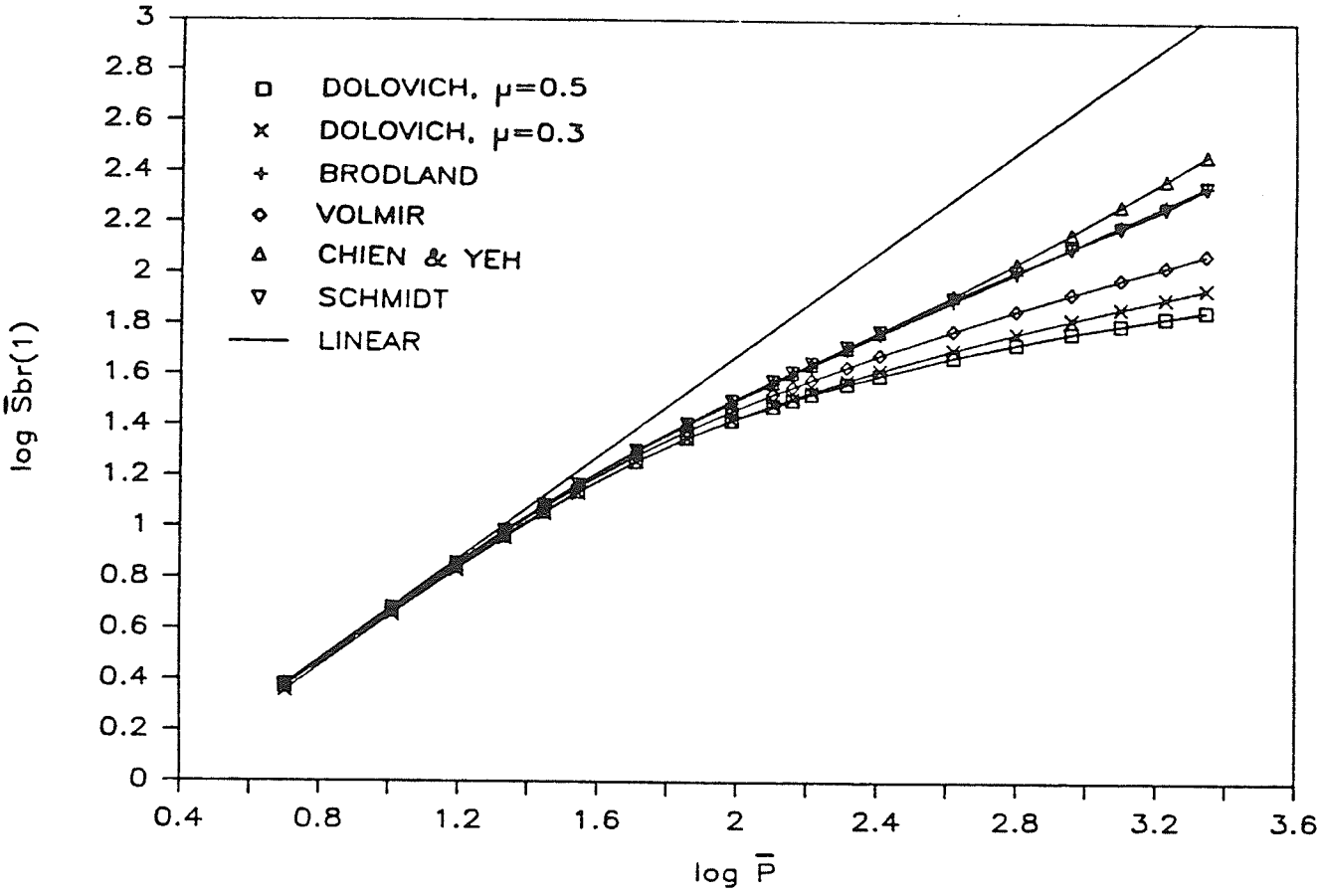

Figure 5.17 Radial Bending Edge Stress Versus Load

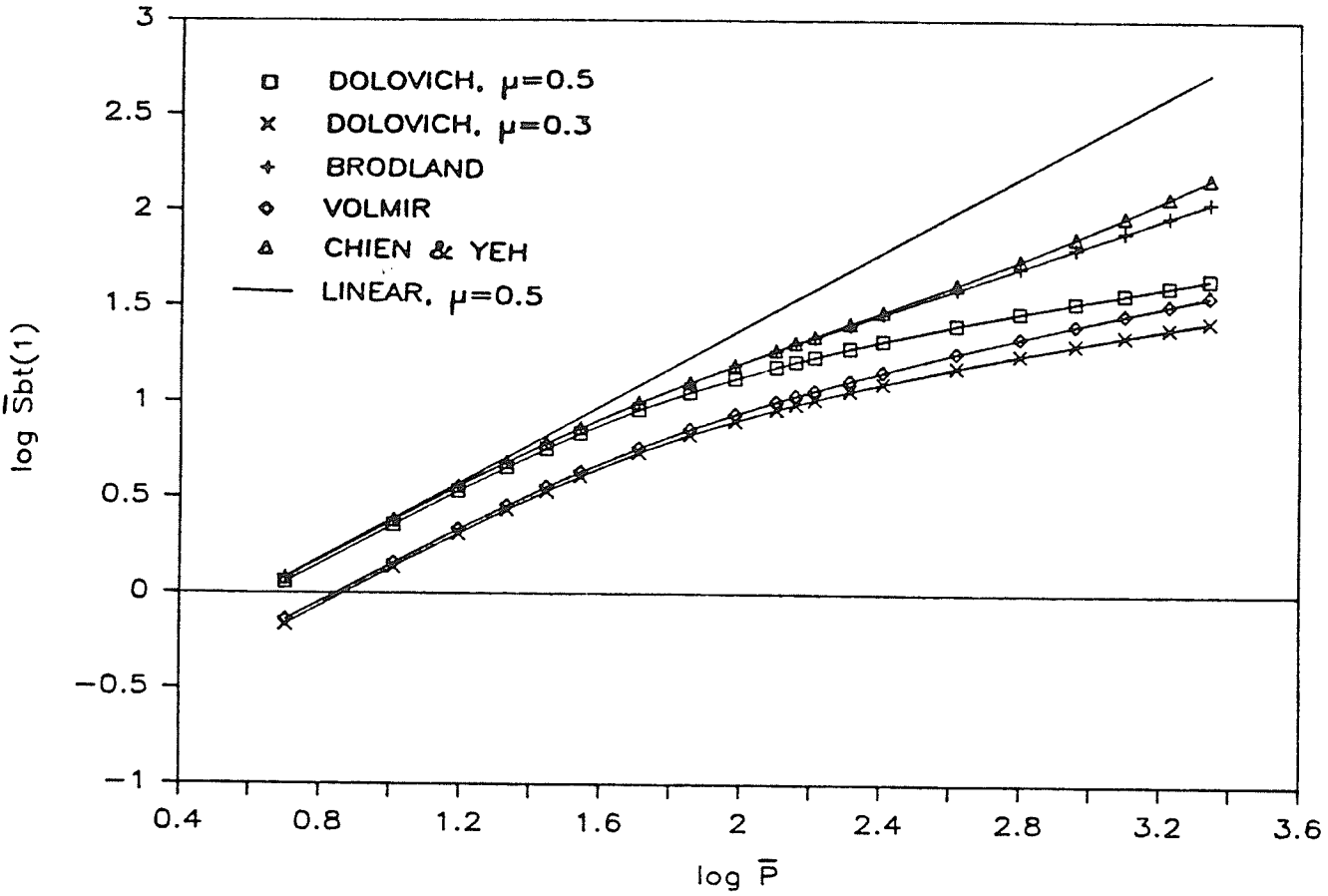

Figure 5.18 Tangential Bending Edge Stress Versus Load

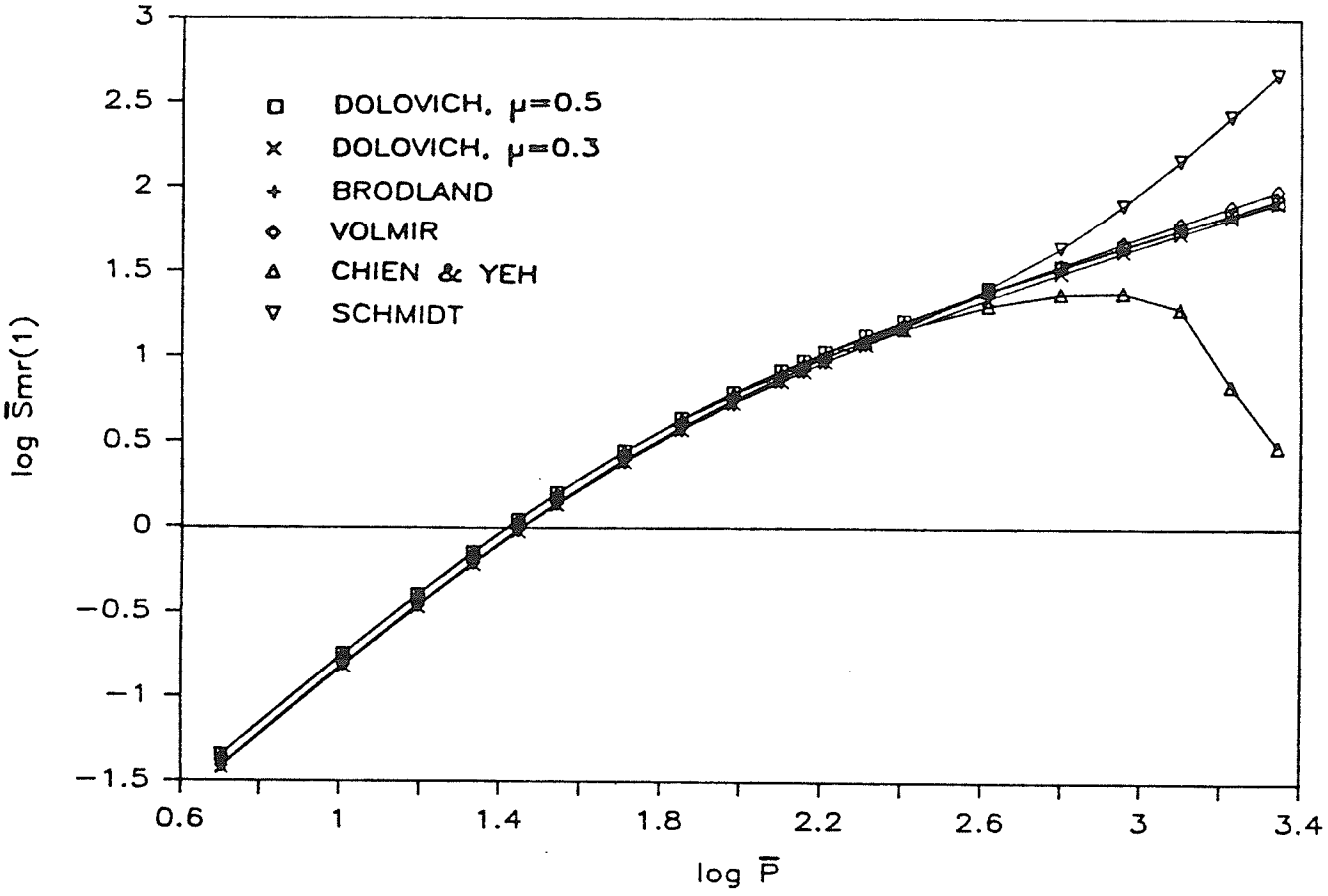

Figure 5.19 Radial Membrane Edge Stress Versus Load

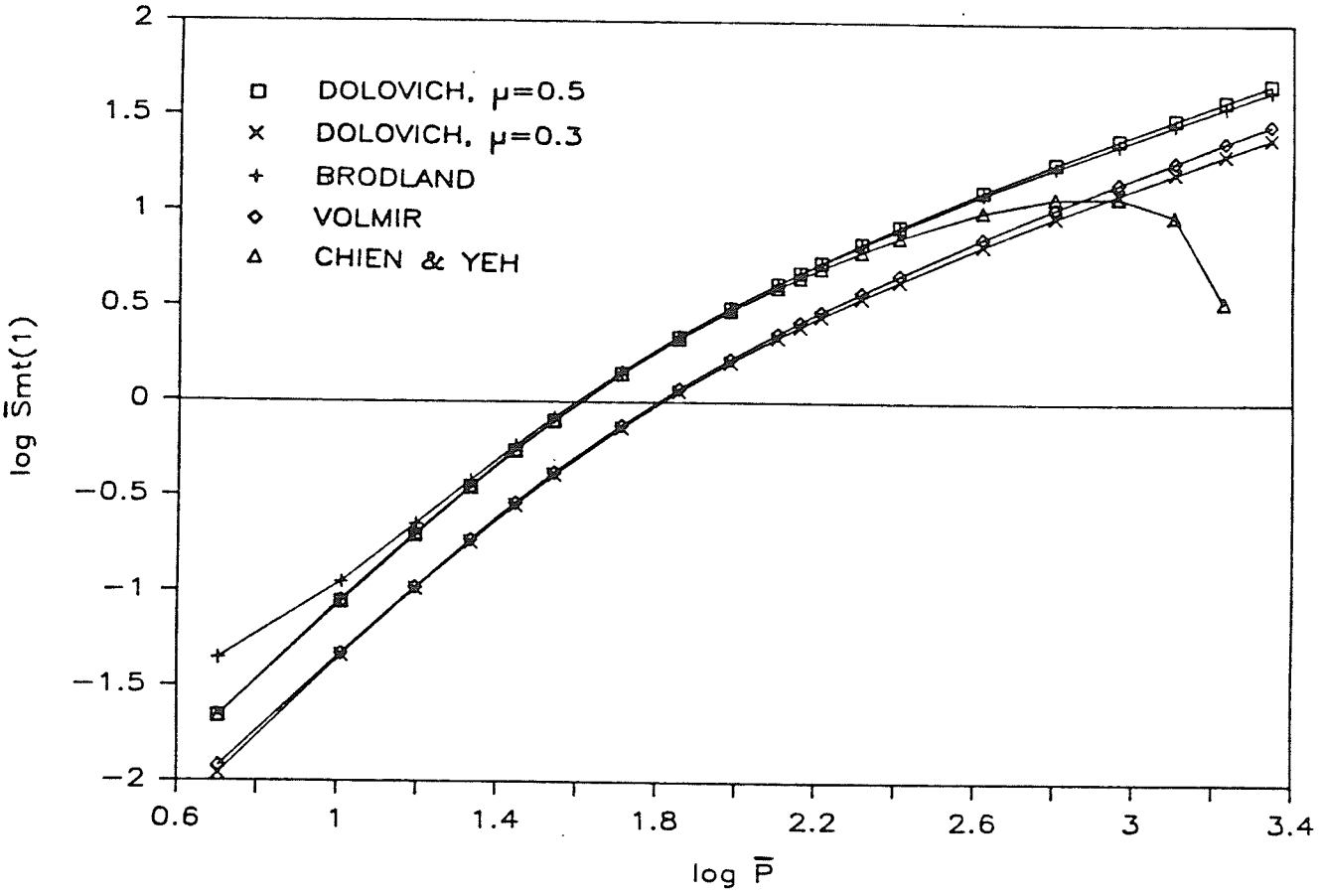

Figure 5.20 Tangential Membrane Edge Stress Versus Load

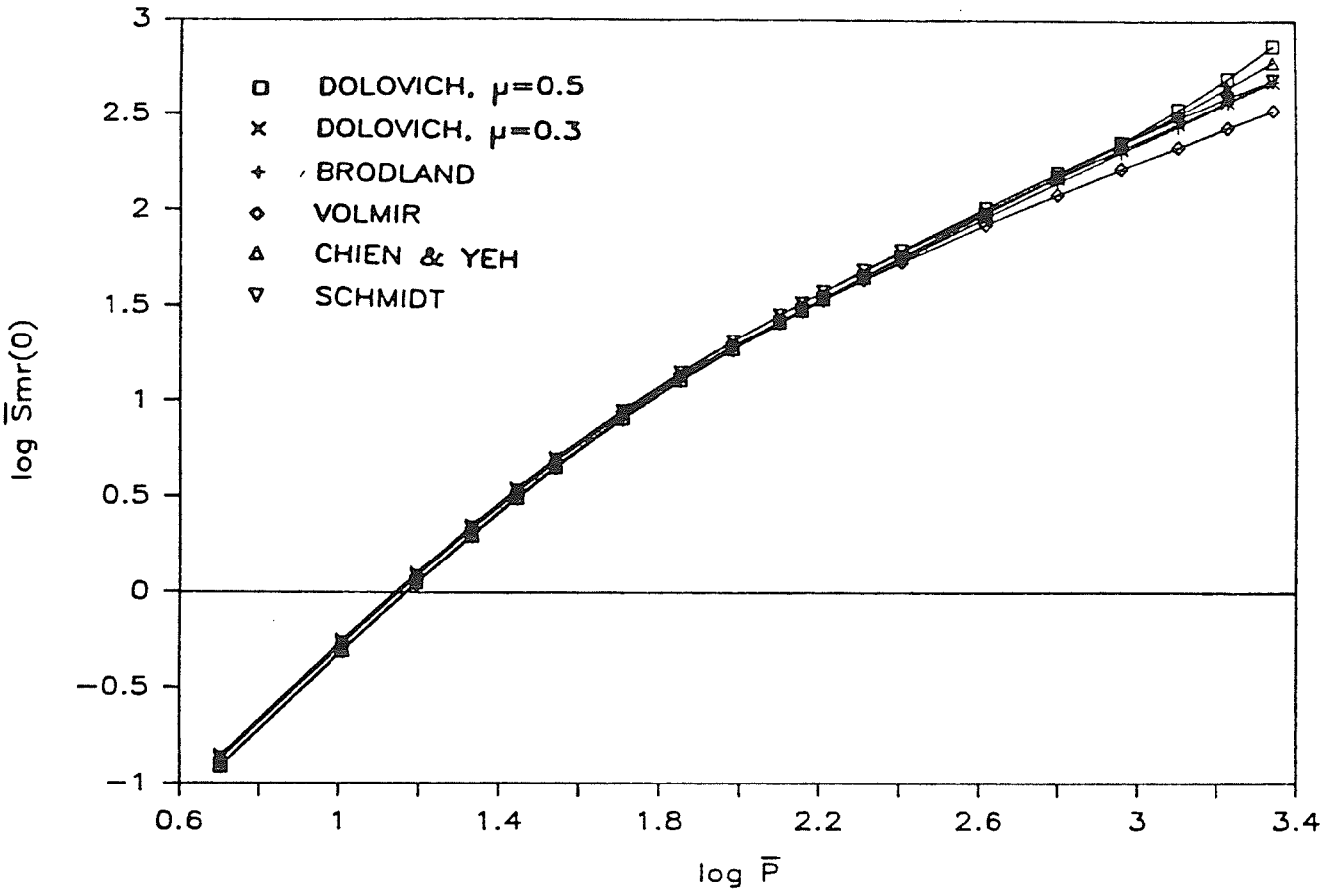

Figure 5.21 Radial Membrane Center Stress Versus Load

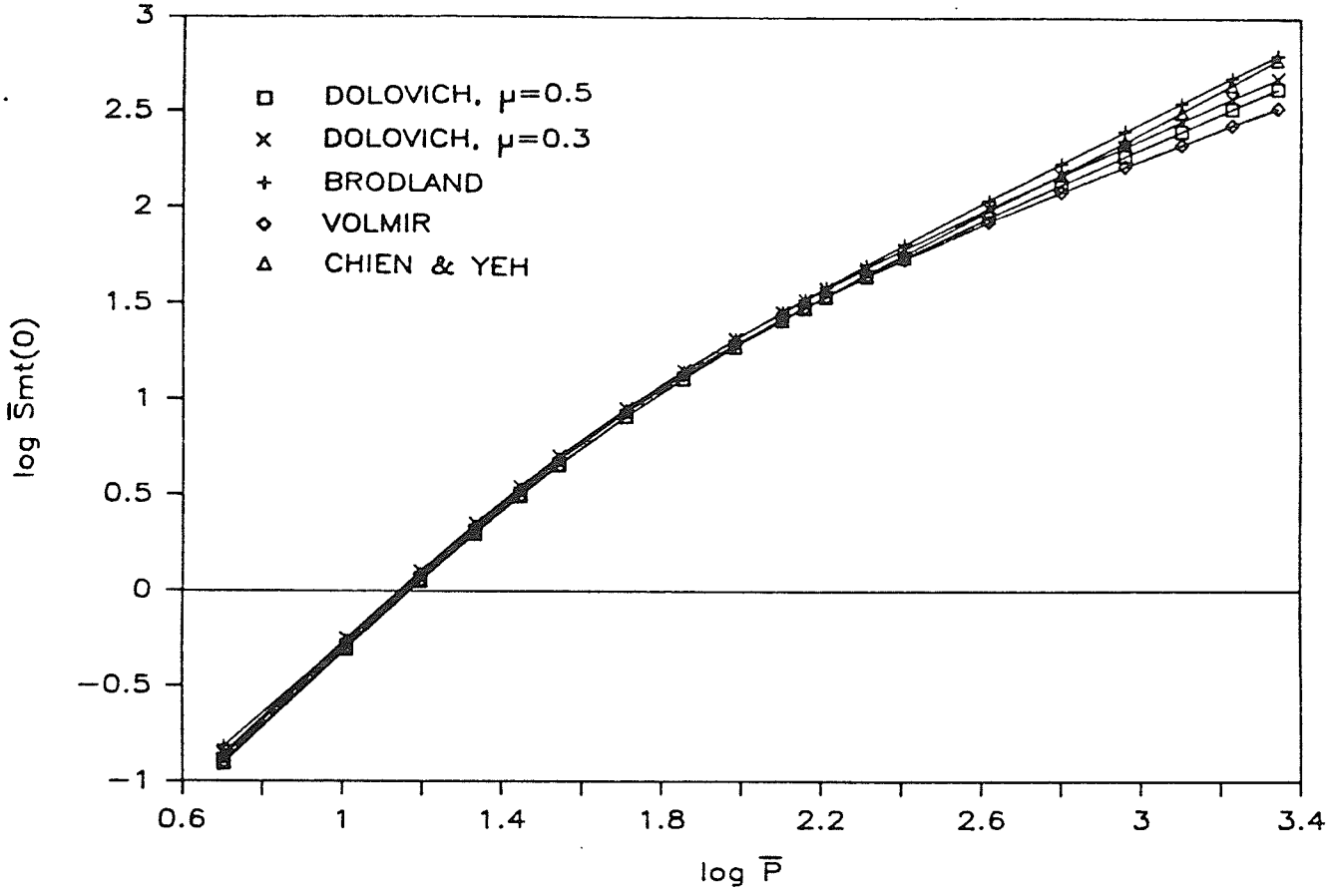

Figure 5.22 Tangential Membrane Center Stress Versus Load

CHAPTER 6

CONCLUSIONS

Starting with Chapter 4, the development constitutes an original contribution to the field of solid mechanics. Specific conclusions regarding the solution characteristics are given on pages 47 and 48 and it is generally concluded that

1) A new approximate solution to the Von Karman equations for a point loaded clamped circular plate has been obtained using a simple nonlinear displacement model.

2) For a given set of input data a, h, E, μ, and A, the prediction of all stresses, strains, and displacements relies on the determination of a single parameter b.

3) A simple empirical formula for b can be used with good results.

4) A further simplified scheme for b can be used for load determination to within $\pm 5\%$ at $4.0<A<5.0$ and accuracy increases as A decreases.

5) The new solution has been shown to have excellent agreement with the literature.

6) Although each advantage offered by the new solution can be found in one or more of the existing analytical results, not one of the other approaches possesses all of the required features. That is, the new solution is
   - simple in form and easy to use
   - general and complete
   - valid for all values of Poisson's ratio
   - accurate over a large range of deflections.

7) The use of shape parameter b allows the formulation to predict the linear case as well as the nonlinear cases.

8) The description of the plate's transverse displacement profiles for large deflections constitutes a considerable improvement over those given by other analytical solutions. Consequently, the introduction of the nonlinear displacement model has provided new insight into the large deflection of point loaded circular plates.

REFERENCES

[1] Brodland, G.W., "Large Axisymmetric Deformation of Thin Shells of Revolution, " Ph.D. Thesis, Department of Civil Engineering, University of Manitoba, Winnipeg, Manitoba, 1985.

[2] Brodland, G.W., "Large Deflection of Uniformly Loaded Circular Plates," Appl. Mech. Rev., in press.

[3] Von Karman, T.,"Festigkeitsprobleme im Maschinenbau," Enzyklopaedie der mathematischen Wissenschaften, Teubner-Verlag, Leipzig, Germany, Vol. 4, 1910, pp. 348-352.

[4] Volmir, A.S., Flexible Plates and Shells, Moscow, 1956.

[5] Timoshenko, S., Woinowsky-Krieger, S., Theory of Plates and Shells, McGraw-Hill Book Company, New York, 1959.

[6] Lukasiewicz, S., Local Loads in Plates and Shells, Sijthoff and Noordhoff, Alphen aan den Rijn, The Netherlands.

[7] Volterra, E., and Gaines, J.H., Advanced Strength of Materials, Prentice-Hall Inc.,Englewood Cliffs, 1971.

[8] Cherepy, R.D., "Large Deflection of a Circular Plate Subjected to a Concentrated Load at the Center," Masters Thesis, University of Arizona, Tuscon, Ariz., 1960.

[9] Stippes, M., and Hausrath, A.H., "Large Deflections of Circular Plates," Journal of Applied Mechanics, ASME, Vol. 19, No. 3, Transactions, Vol. 74, Sept., 1952, pp. 287-292.

[10] Chien, W.Z. and Yeh, K.Y., "On the Large Deflection of Circular Plates," Scientia sin., Vol. 3, 1954, pp. 405-436.

[11] Schmidt, R., "Large Deflections of a Clamped Circular Plate," Journal of Engineering Mechanics, Division ASCE, Vol. 94, Dec. 1968, pp. 1603-1606.

[12] Chia, C.Y., Nonlinear Analysis of Plates, McGraw-Hill, New York, 1980.

[13] Basuli, S., "Note on the Large Deflection of a Circular Plate Under a Concentrated Load,"Zeitschrift fuer angewandtke Mathematik und Physik, Switzerland, Vol. 12, July, 1961, pp. 357-362.

[14] Berger, H.M., "A New Approach to the Analysis of Large Deflections of Plates," J. Appl. Mech., Vol. 22, 1955, pp. 465-472.

[15] Jahsman, W.E., Field, F.A., and Holmes, A.M.C., "Finite Deformations in a Prestressed, Centrally loaded, Circular Elastic Membrane," Proc. Fourth (U.S.) National Congress of Applied Mechanics, Vol.1, Berkeley, 1962, pp. 585-594.

[16] Frakes, J.P., and Simmonds, J.G., "Asymptotic Solutions of the Von Karman Equations for a Circular Plate Under a Concentrated Load," Transactions of the ASME, Vol.52, June 1985, pp. 326-330.

[17] Saibel, E., and Tadjbakhsh, I., "Large Deflections of Circular Plates Under Uniform and Concentrated Central Loads," ZAMP, Vol. 11, 1960, pp. 497-503.

[18] Way, S., "Bending of Circular Plates with Large Deflection," Transactions, ASME, Vol. 56, 1934, pp. 627-636.

[19] Trim, D.W., Calculus and Analytic Geometry, Addison-Wesley, Don Mills, 1983.

[20] Stoecker, W.F., Design of Thermal Systems, McGraw-Hill Book Company, New York, 1980.

[21] McFarland, D., Smith, B.L., and Bernhart, W.D., Analysis of Plates, Spartan Books, New York, 1972.